Effects of Hydroxychloroquine and Azithromycin on iPSC-derived Cardiomyocytes: Considerations for the Treatment of COVID-19 Patients

Wener Li[a,§], Xiaojing Luo[a,§], Mareike S. Poetsch[a], Reinhard Oertel[b], Kapil Nichani[c], Martin Schneider[c], Anna Strano[a], Marcel Hasse[a], Robert-Patrick Steiner[a], Lukas Cyganek[d,e], Karina Hettwer[c], Steffen Uhlig[c], Kirsten Simon[c], Kaomei Guan[a,*], Mario Schubert[a,*]

[a] Institute of Pharmacology and Toxicology, Technische Universität Dresden, Germany

[b] Institute of Clinical Pharmacology, Technische Universität Dresden, Germany

[c] QuoData – Quality & Statistics GmbH, Dresden, Germany

[d] Clinic for Cardiology and Pneumology, University Medical Center Göttingen, Germany

[e] DZHK (German Center for Cardiovascular Research), partner site Göttingen, Germany

[§] These authors contributed equally to this work.

* MSchu and KG share senior authorship.

* Corresponding author:

Prof. Dr. Kaomei Guan

Institute of Pharmacology and Toxicology

Technische Universität Dresden

Fetscherstraße 74

01307 Dresden, Germany

Tel: (+49)3514586246

Fax: (+49)3514586315

E-mail: kaomei.guan@tu-dresden.de

Abstract

Despite known adverse effects of hydroxychloroquine (HCQ) and azithromycin (AZM) on cardiac function, HCQ and AZM have been used as combination therapy in the treatment of COVID-19 patients. Recent clinical data indicate higher complication rates with HCQ/AZM combination treatment in comparison to monotherapy. Here, we used human induced pluripotent stem cell-derived cardiomyocytes (iPSC-CMs) to systematically investigate the effects of HCQ and AZM individually and in combination. The clinically observed QT prolongation caused by treatment with HCQ could be recapitulated in iPSC-CMs based on prolonged field potential duration (FPDc). Interestingly, HCQ-induced FPDc prolongation was strongly enhanced by combined treatment with AZM, although AZM alone slightly shortened FPDc in iPSC-CMs. Furthermore, combined treatment with AZM and HCQ leads to higher cardiotoxicity, more severe structural disarrangement, and more pronounced contractile and electrophysiological dysfunctions, compared to respective mono-treatments. First mechanistic insights underlying the synergistic effects of AZM and HCQ on iPSC-CM functionality are provided based on increased Cx43- and Nav1.5-protein levels. Taken together, our results highlight that combined treatment with HCQ and AZM strongly enhances the adverse effects on cardiomyocytes, providing mechanistic evidence for the high mortality in patients receiving HCQ/AZM combination treatment.

Keywords: COVID-19; hydroxychloroquine; azithromycin; field potential duration; conduction velocity; human induced pluripotent stem cells; cardiomyocyte; drug testing

Introduction

The severe acute respiratory syndrome coronavirus 2 (SARS-CoV-2) has caused a worldwide pandemic. Several anti-viral drugs have been considered to improve clinical outcomes, including hydroxychloroquine (HCQ), remdesivir, and lopinavir[1]. Attempts using HCQ in combination with azithromycin (AZM) reported first positive results for the treatment of SARS-CoV-2 infected (COVID-19) patients, demonstrating reinforced viral load reduction/disappearance in a small number of COVID-19 patients[2, 3]. However, this study has been frequently criticized, because following clinical trials and the meta-analyses could not confirm the efficacy of treatment with HCQ or HCQ in combination with AZM[1, 4, 5]. Moreover, side effects on cardiovascular function have been widely observed during long-term HCQ/AZM combination therapy[6, 7].

Chloroquine (CQ) and HCQ are widely used antimalarial medications and known to inhibit the replication of viruses *in vitro*[8]. Conduction disorders were reported to occur in 85% of patients after chronic treatment with HCQ (or CQ) and represent one of the main side effects of HCQ[9, 10]. Mechanistic insights from animal models revealed that acute application of HCQ reduces the heart rate by modulating the funny current I_f[11, 12].

AZM, a broad-spectrum macrolide antibiotic, was considered a good safety profile until the report of a small absolute increase in cardiovascular deaths during 5 days of AZM therapy[13]. In addition, several cases of AZM-induced QT-interval prolongation were reported in the clinic[12, 14].

A retrospective multicenter study by Rosenberg *et al.* confirmed that the combination therapy of HCQ and AZM not only potentiated the risk for cardiac arrest, but is further associated with an increased mortality rate[15]. In line with these findings, Wang *et al*. showed that the treatment with combined HCQ and AZM, but not HCQ or AZM alone, enhanced the susceptibility for ventricular arrhythmias[16]. QT interval prolongation, as reported by various groups[17, 18, 19, 20], must be considered as an additional adverse effect for COVID-19 patients resulting from the HCQ and AZM combination therapy. As the mechanisms underlying HCQ and AZM-related cardiac synergistic effects are not fully understood, the benefit-risk balance between the treatment of COVID-19 patients with such compounds and potential cardiac side effects remains a dilemma for physicians.

The aim of the study was to investigate the effects of HCQ, AZM, and their combination, in a clinically relevant concentration range and treatment duration, to better understand their arrhythmia-inducing mechanisms in an *in vitro* human cardiomyocyte model system. The use of induced pluripotent stem cell-derived cardiomyocytes (iPSC-CMs) in this study offered a robust platform to investigate the consequences of HCQ and AZM treatment on the viability, the contractile structure, and on contractility and electrophysiology of human cardiomyocytes.

Results

This study was designed to characterize the effects of HCQ and AZM alone or in combination on iPSC-CMs and to investigate the underlying mechanistic basis for the increased complication rates with combination therapy. The concentrations were chosen based on previously reported plasma concentrations of the drugs in patients. In the treatment of COVID-19, the drugs were administrated to patients for 5-10 days. Thus, in this study, iPSC-CMs from 4 different donors (1-2 iPSC lines each) without known cardiovascular disease were treated with HCQ (1, 3, and 10 µM), AZM (1 and 10 µM) or their combination for 7 days (Supplementary Figure 1). Afterward, they were cultured for another 7 days without the drugs (washout period).

Effects of HCQ and AZM on cell morphology and viability

First, the effects of HCQ and AZM on the morphology of iPSC-CMs were investigated. Treatments with AZM and HCQ, in particular at higher concentrations, caused the formation of vesicle-like structures within the cells (Figure 1A), which persisted till 7 days after drug washout (Figure 1D). Overview images (Figure 1A) and cell nucleus counting (Supplementary Figure 2) showed reduction in total cell number after 7 days of the combination treatment with 10 µM HCQ and 10 µM AZM. Importantly, treatment with vehicle had no influence on viability or cell number (Supplementary Figure 3A-C). Cells treated with 10 µM HCQ alone or in combination with 1 µM AZM showed a progressive cell death (Figure 1D). The MTT assay revealed that 7-day combination treatment with 10 µM HCQ and 10 µM AZM led to less than 50% of cells at a viable and metabolically active state (Figure 1B), whereas HCQ (1 µM or 3 µM) alone or in combination with AZM (1 µM or 10 µM), respectively, did not significantly affect metabolic activity of iPSC-CMs (Figure 1B). Significantly higher rates of cell death were also observed as indicated by increased lactate dehydrogenase (LDH) activity in the cell supernatant in the groups treated with 10 µM HCQ in combination with AZM (1 µM or 10 µM) (Figure 1C). In contrast to HCQ, 10 µM AZM alone showed no effect on cell viability using both MTT and LDH activity assays (Figure 1B, C). After 7-day drug washout, the cytotoxic effect of 10 µM HCQ became more evident. The MTT assay revealed a further decrease in viability of cells treated with 10 µM HCQ alone or in combination with 1 µM AZM, which was consistent with reduced cell confluency (Figure 1D, E). Notably, due to significantly reduced cell numbers in groups treated with 10 µM HCQ alone or in combination with AZM as well as the daily medium change, LDH activity in the supernatant is not representative in these samples after the drug washout (Figure 1F). Treatment of cells with lower drug concentrations (1 or 3 µM HCQ, 1 or 10 µM AZM) did not affect cell viability (Figure 1E and F). These results demonstrate the high toxicity of HCQ at higher concentrations, which is further increased in the presence of AZM.

Figure 1

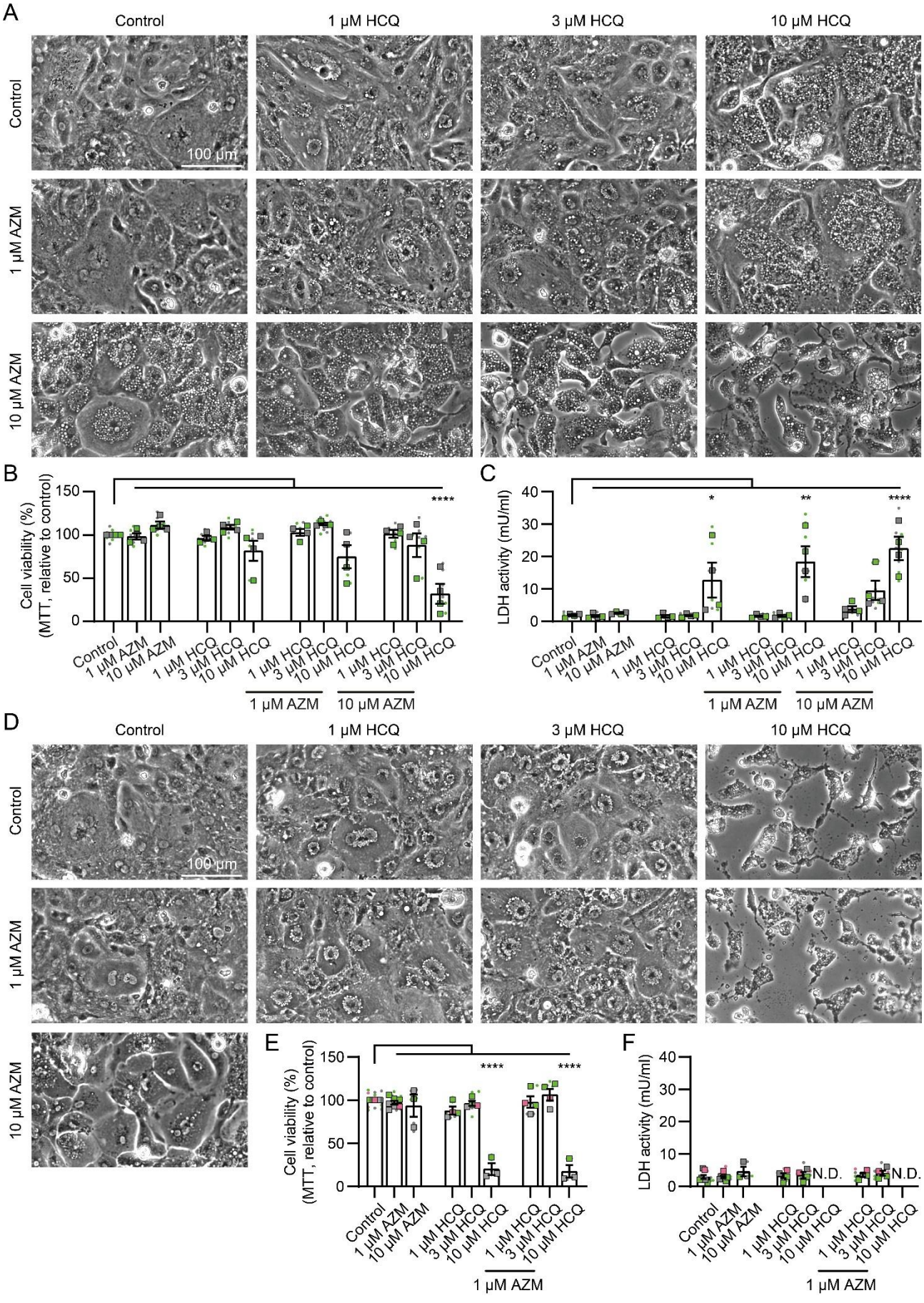

Figure 1: Morphological changes and cytotoxicity in iPSC-CMs treated with HCQ and AZM. A, Representative brightfield images depicting morphology of iPSC-CMs after 7-day treatments with HCQ and AZM in different concentrations. Scale bar: 100 µm. B, Cell viability after 7-day drug treatment as determined by measurement of formazan formation in the MTT assay. C, LDH activity detected in cell supernatants after 7-day drug treatment. D, Representative brightfield images depicting morphology of iPSC-CMs after 7-day drug treatment and 7-day washout period. Even after washout, iPSC-CMs treated with a combination of high concentrations of AZM and HCQ show severe morphological changes and increased cell death. Scale bar: 100 µm. E, Cell viability after 7-day drug washout as determined by using the MTT assay. F, LDH activity detected in supernatants after 7-day drug washout. Data represent technical replicates (points) and means (squares) of each experiment, N = 3-7 independent experiments using iPSC-CMs from 3 healthy donors (iBM76.1, iBM76.3 in green; iWTD2.1, iWTD2.3 in grey, isWT7.22 in pink). Lines and errors show overall mean and SEM. Statistical analysis was performed using one-way ANOVA and Tukey's multiple comparison test. ** $p < 0.01$, **** $p < 0.0001$. N.D. – not determined.

HCQ and AZM affect the structural organization of iPSC-CMs

To investigate the effects of HCQ and AZM on iPSC-CM area, sarcomere organization and sarcomere length, we performed immunofluorescence staining to detect α-actinin. To evaluate the effect of AZM and HCQ on cell area, iPSC-CMs were seeded at low density to monitor single cells. Single cells were less resistant to drug treatment compared to cells in monolayer by showing severe morphological changes and cell death, in particular, under treatment with 10 µM HCQ and 10 µM AZM either alone or in combination (Figure 2A). Therefore, structural analyses of iPSC-CMs were only performed for treatments with lower drug concentrations, for which cell detachment was less evident.

The 7-day treatment with 1 µM AZM alone resulted in an increase in cell area (Figure 2B). The observed increase in cell area after the 7-day treatment with 1 µM AZM did not persist after washout, but with a slight decrease (Figure 2C). After 7-day treatment with 3 µM HCQ alone, iPSC-CMs showed a reduction in cell area, which was not obvious in the groups treated with 1 µM HCQ alone or with HCQ (1 and 3 µM) in combination with 1 µM AZM (Figure 2A and B). However, after the drug washout, iPSC-CMs treated with 1 and 3 µM HCQ alone or in combination with 1 µM AZM showed smaller cell areas compared to control cells, indicating persistent cellular shrinking (Figure 2C).

To quantify the effect of HCQ and AZM on sarcomeric organization in iPSC-CMs, the proportion of cells with structurally organized and disorganized sarcomeres were manually determined based on the images of iPSC-CMs stained for α-actinin. Cells with evenly distributed intact sarcomeres

155 across the cell body (occupying > 80% of the cell area) were classified as structurally organized
156 (Figure 2D, left), while cells with intact sarcomeres distributed exclusively in the center or cell
157 periphery and cells lacking clearly organized ladder-like sarcomeres were classified as structurally
158 disorganized (Figure 2D, right). Under basal conditions, 61 ± 6% of iPSC-CMs were classified as
159 structurally organized (Figure 2E). The relatively high portion of cells with disorganized sarcomeres
160 at basal condition might result from the immaturity of iPSC-CMs undergoing sarcomere assembly.
161 Treatment with 1 µM AZM and 1 µM HCQ alone revealed no effect on the sarcomere organization
162 of iPSC-CMs. An increase in the percentage of structurally disorganized cells was found in cells
163 treated with 3 µM HCQ alone ($p = 0.055$) or in combination with 1 µM AZM ($p < 0.0001$, Figure 2E).

164 As another important aspect of iPSC-CM structure, the sarcomere length was measured in the
165 population of structurally organized cells (Figure 2D, left). The sarcomere length of iPSC-CMs at
166 basal condition was determined as 2.04 ± 0.05 µm, which is comparable to a sarcomere length of
167 ~2.2 µm observed in mature cardiomyocytes[21]. After 7-day treatment with 1 µM AZM, 3 µM HCQ,
168 or the combination of HCQ (1 and 3 µM) and 1 µM AZM, iPSC-CMs showed a significant reduction
169 in sarcomere length, which was not obvious in the group treated with 1 µM HCQ alone (Figure 2F).
170 The strongest reduction in sarcomere length was observed in the group treated with 1 µM AZM
171 combined with 3 µM HCQ, which demonstrates the negative effects of both compounds on the
172 organization of the contractile structures. After the subsequent washout period for 7 days,
173 sarcomere length remained strongly reduced in groups treated with 3 µM HCQ alone and HCQ in
174 combination with AZM and slightly reduced in iPSC-CMs treated with 1 µM AZM or 1 µM HCQ
175 alone (Figure 2G).

176 Taken together, these results highlight the negative effect of HCQ and AZM treatments on the
177 structural characteristics of iPSC-CMs and the persistence of their adverse effects even after drug
178 washout for 7 days.

Figure 2

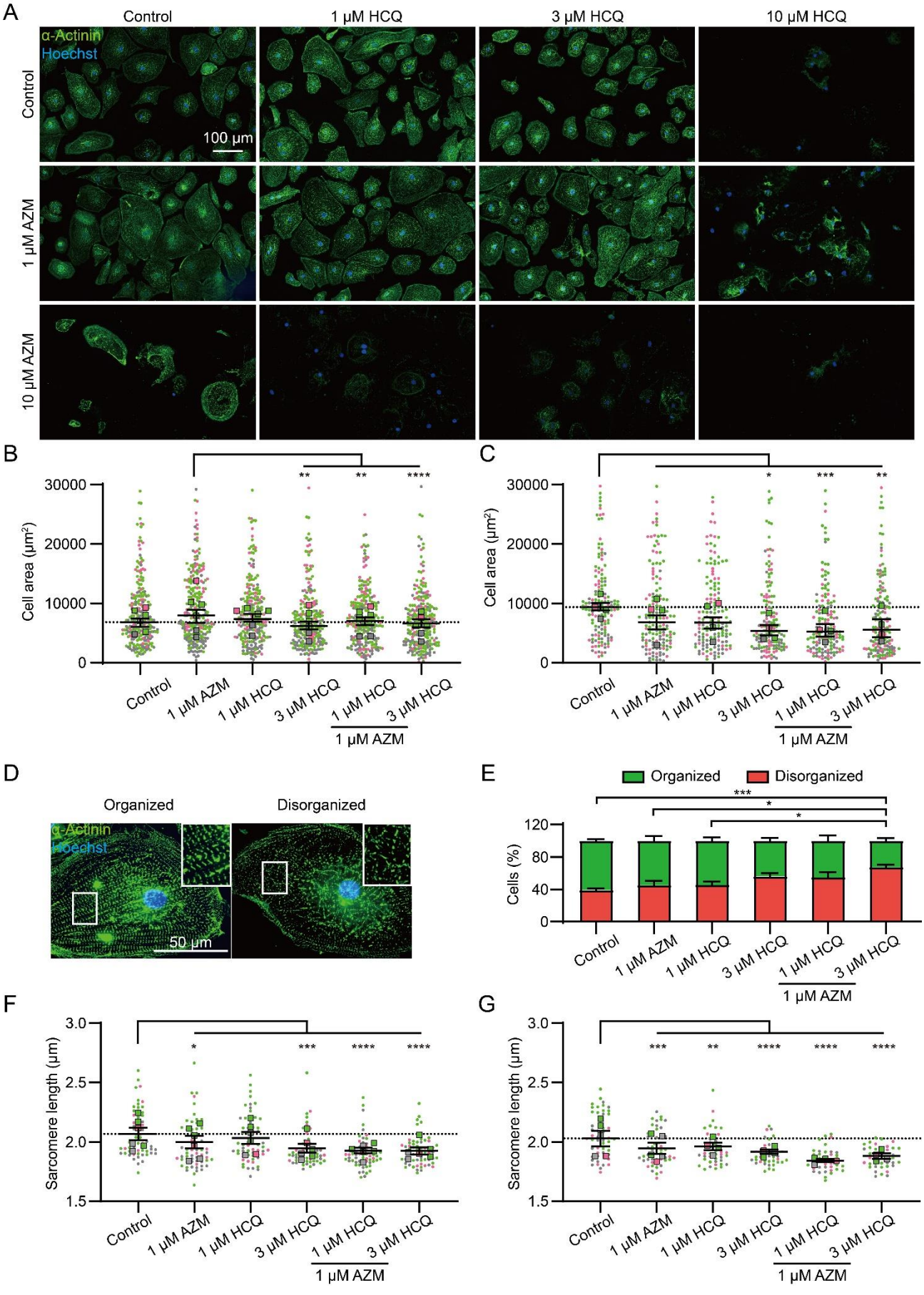

Figure 2: HCQ and AZM cause sarcomeric disorganization in iPSC-CMs. A, Representative images of α-actinin immunostained iPSC-CMs treated with different concentrations of HCQ and AZM for 7 days. B-C, Analysis of cell areas after 7-day drug treatment (B) and after subsequent 7-day washout (C). A total of n = 160-240 cells (40 per experiment) from 6 (B) or 4 (C) independent experiments per condition were analyzed. Points represent values of single cells and squares the median values of individual experiments. Lines indicate median and 95% CI of the overall population. D, Representative images of structurally organized and disorganized iPSC-CMs after drug treatment for 7 days. E, Percentage of structurally organized and disorganized iPSC-CMs after 7-day drug treatment. Mean and SEM of 5 independent experiments (n = 96-272 cells analyzed per condition from each experiment) are shown. F-G, Sarcomere length after 7-day drug treatment (F) and after 7-day washout (G). Mean and SEM of n = 40-60 cells (10 per experiment) from 6 (F) or 5 (G) independent experiments are shown. Data plots in F, and G show technical replicates (dots) and mean values (squares). Colors indicate iPSC-CM differentiations from 3 healthy donors (iBM76.1, iBM76.3 in green; iWTD2.1, iWTD2.3 in grey, isWT7.22 in pink). Statistical analysis was performed using one-way ANOVA and Tukey's multiple comparison test. ** $p < 0.01$, *** $p < 0.001$, **** $p < 0.0001$.

HCQ and AZM alter the contractility of iPSC-CMs

The effects of HCQ and AZM on the beating property of iPSC-CMs were investigated using video-based motion vector analysis (Supplementary Figure 4A). This method allows the quantification of specific parameters of contraction and relaxation[22, 23]. As a quality control, all beating parameters remained unchanged for cells cultured with 0.1% DMSO (vehicle) during the 7-day treatment (Supplementary Figure 3). A progressive alteration of cardiomyocyte beating properties was observed in the presence of AZM and HCQ during the 7-day treatment period (Figure 3, Supplementary Figure 4B-G, Supplementary Videos 1, 2). While AZM (1 µM) and HCQ (1 µM and 3 µM) alone had no or less effect on the beating parameters of iPSC-CMs during the 7-day treatment (Figure 3B-E), strong changes were observed in iPSC-CMs treated with AZM (10 µM) and HCQ (10 µM) alone or with AZM (1 and 10 µM) in combination with HCQ (1, 3 and 10 µM) (Figure 3B-E, Supplementary Figure 4B-G). Notably, treatment with 10 µM HCQ alone or in combination with 1 µM or 10 µM AZM led to stop of beating or strongly distorted motion in some cultures of iPSC-CMs, which could not be included in the analysis (Figure 3A, B). With respect to beating rate (Figure 3B, Supplementary Figure 4B), iPSC-CMs treated with 10 µM AZM alone showed an increase in beating rate at day 1 but a decrease at day 7 (Supplementary Figure 4B, Figure 3B), while 10 µM HCQ alone progressively increased the beating rate of iPSC-CMs from day 1 onwards (Figure 3B, Supplementary Figure 4B). A combination of AZM (1 or 10 µM) with 10 µM HCQ led to even higher beating rates than 10 µM HCQ alone (Figure 3B). Moreover, an

increased beating rate was also observed in the group treated with 3 µM HCQ in combination with 10 µM AZM, which was absent in the cells treated with 3 µM HCQ alone (Figure 3B). In terms of contraction time and relaxation time, 10 µM AZM alone showed a progressive reduction, similar to the group treated with 10 µM HCQ alone during the 7-day treatment (Figure 3C and D, Supplementary Figure 4D and F). The combination of HCQ and AZM enhanced the decrease of contraction and relaxation time in a concentration- and time-dependent manner (Figure 3C and D). Of note, the combination of 10 µM AZM with only 1 µM and 3 µM HCQ led to a further reduction in contraction and relaxation time.

Overall, these data demonstrate that AZM and HCQ directly affect beating rate, as well as contraction and relaxation behavior of iPSC-CMs in a concentration- and time-dependent manner, while the combination of AZM with HCQ enhances the effects of HCQ on raising the beating rate of iPSC-CMs as well as on decreasing contraction time and relaxation time.

Figure 3

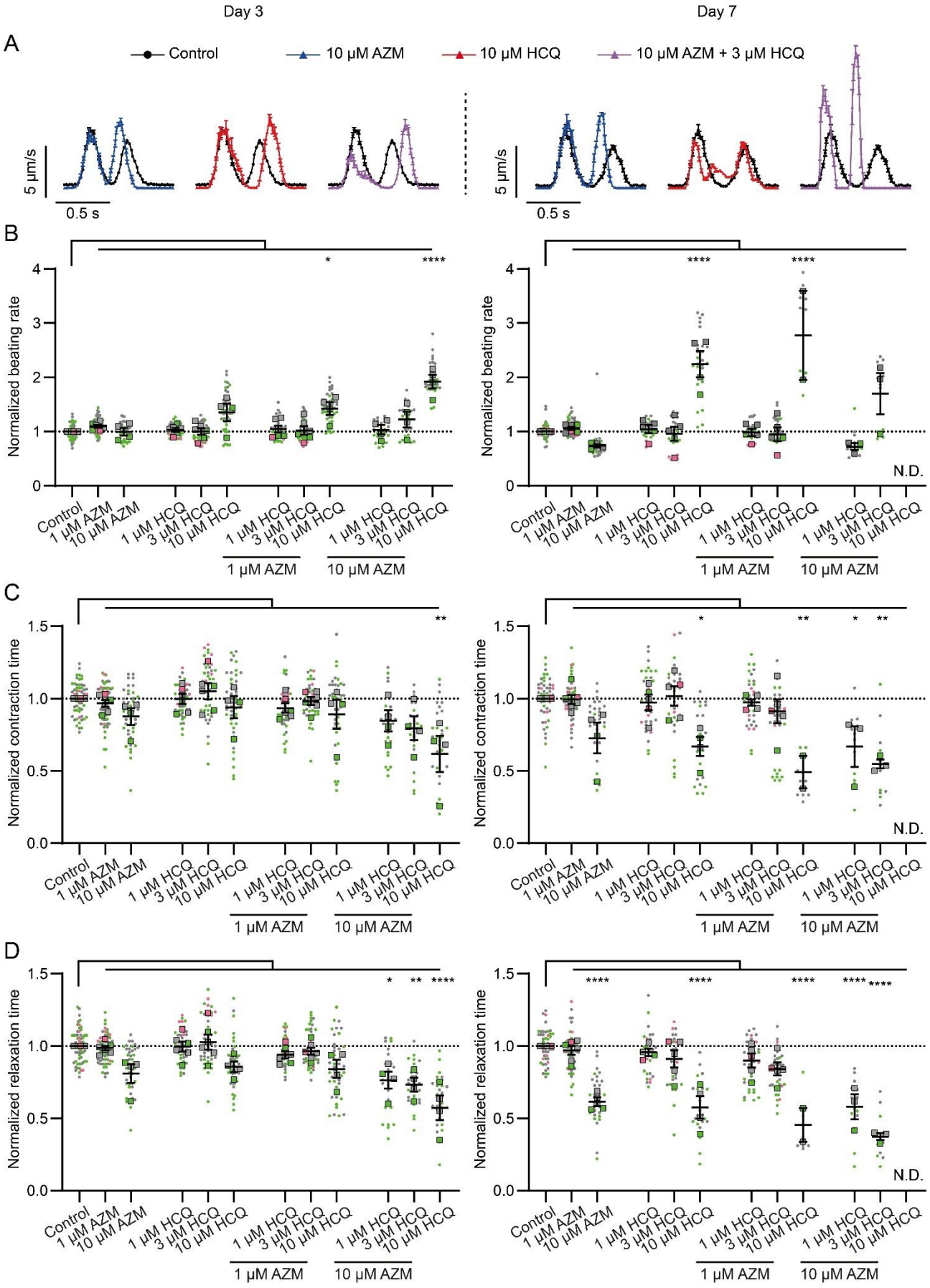

Figure 3: Contractile dysfunctions in iPSC-CMs treated with HCQ and AZM. A, Representative motion traces observed in iPSC-CMs using vector-based quantification on treatment days 3 (left) and 7 (right). Values represent mean and SEM of motions from aligned contraction-relaxation cycles of a representative video. B-D, Effects of AZM and HCQ alone as well as their combination on the beating rate (B), contraction time (C) and relaxation time (D) on treatment day 3 (left) and 7 (right). Data represent technical replicates (points, n = 9-54 videos per condition) and means (squares) of each experiment, N = 4-6 independent experiments using iPSC-CMs from 3 healthy donors (iBM76.1, iBM76.3 in green; iWTD2.1, iWTD2.3 in grey, isWT7.22 in pink). Due to the high toxic effects of HCQ or AZM at higher concentrations or in combination, fewer videos could be analyzed under these conditions. Lines show overall mean values and SEM. Statistical analysis based on the mean values of the individual experiments using one-way ANOVA and Tukey's multiple comparison test. * $p < 0.05$, ** $p < 0.01$, *** $p < 0.001$, **** $p < 0.0001$.

HCQ and AZM lead to the prolongation of field potential duration in iPSC-CMs

To assess the effect of HCQ and AZM on the heart rhythm, the field potential (FP) analysis in iPSC-CMs were performed using the multi-electrode array (MEA) technique. As shown in Figure 4A and B, the corrected FP duration (FPDc) in the control group remained stable while 1 µM AZM showed no effect on the FPDc during the 14-day recording (7-day drug treatment and subsequent 7-day washout). However, 10 µM AZM slightly shortened the FPDc of iPSC-CMs, and drug washout could not restore it to the basal level (Figure 4A and B). Treatment with HCQ at low concentrations (1 µM and 3 µM) had no effect on FPDc, however, iPSC-CMs treated with 10 µM HCQ showed a prolonged FPDc from day 2, which kept rising until day 7 (Figure 4A and C). The prolongation of FPDc induced by 10 µM HCQ was reversible, as drug washout gradually eliminated this effect.

When 1 µM AZM was combined with HCQ (1, 3 or 10 µM), similar effects as HCQ alone were observed, showing the prolongation of FPDc only with 10 µM HCQ, but to a lesser extent (Figure 4D). The combination of 10 µM AZM with 3 µM HCQ significantly and reversibly prolonged the FPDc of iPSC-CMs, which was not observed in cells treated with the combination of 10 µM AZM with 1 µM HCQ (Figure 4). When we combined 10 µM AZM with 10 µM HCQ, the prolonged FPDc in iPSC-CMs was observed from day 3 till day 8 (Figure 4E). However, we observed that 55% of iPSC-CMs failed to reveal FP and showed cell death on day 8 (the first day of washout), and 82% of cultures stopped beating at the end of the experiment (Figure 4A, E, Supplementary Figure 5, Supplementary Table 1). In terms of beating frequency, 10 µM AZM caused a significant increase in spontaneous beating frequency on day 1 but a lower beating frequency from day 4 onwards (Supplementary Figure 6A) whereas 10 µM HCQ led to a significant increase from day 1 onwards (Supplementary Figure 6B), which are line with the results observed in the contractility

experiments. Interestingly, most drug-treated iPSC-CMs had a slower beating rate than the control group during the washout period (Supplementary Figure 6).

Figure 4

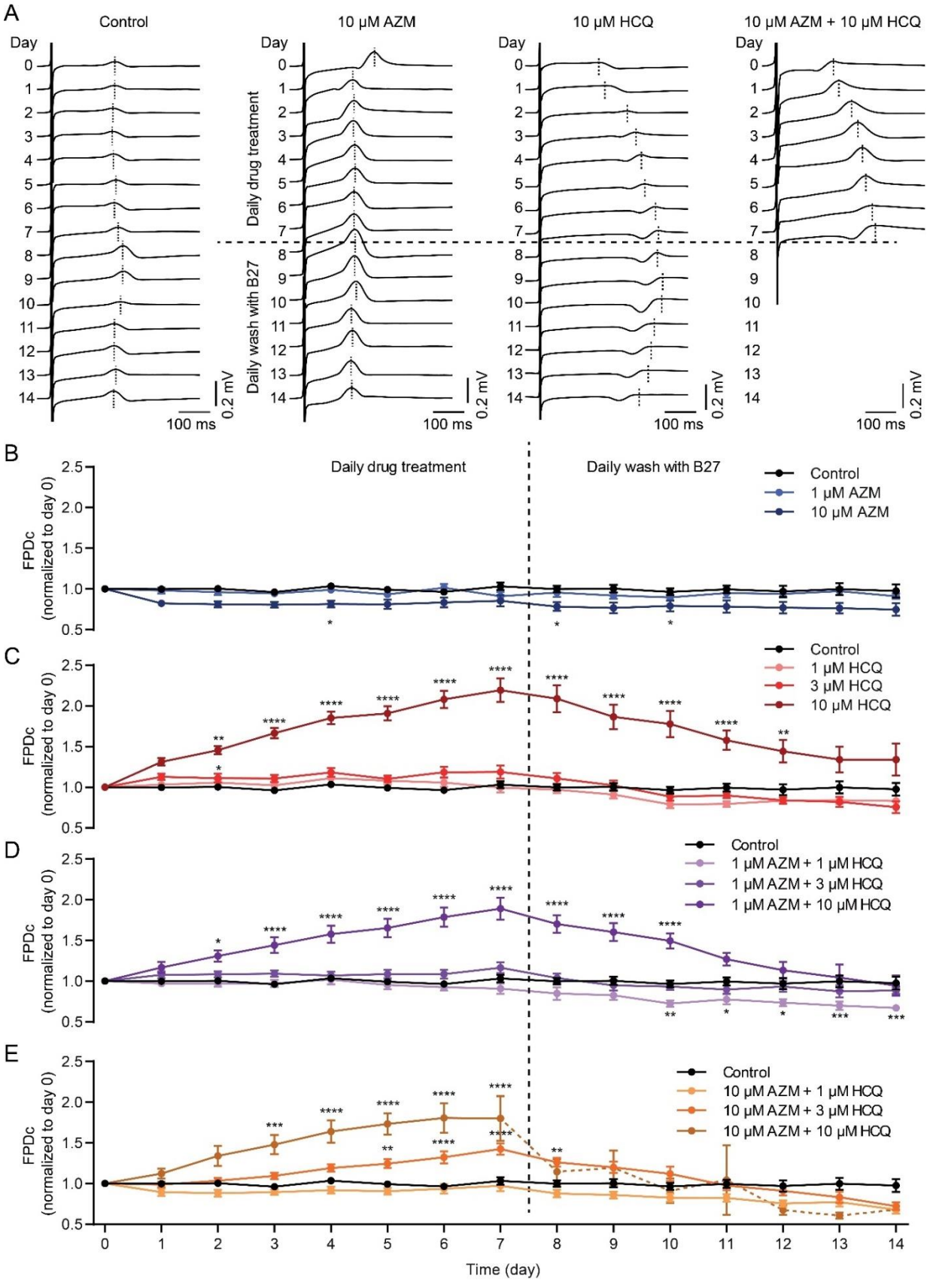

Figure 4: Effects of HCQ and AZM on the field potential duration of iPSC-CMs. A, Representative recordings of extracellular FP in spontaneous beating iPSC-CMs under different treatment conditions. iPSC-CMs treated with 10 µM AZM and 10 µM HCQ in combination stopped beating at day 8 (one day after initiation of washout). B, C, Effect of AZM (B) or HCQ (C) on the corrected FPD (FPDc, normalized to day 0) during 7-day treatment and subsequent 7-day washout. D, E, Effects of HCQ (1, 3 and 10 µM) combined with 1 µM AZM (D) or 10 µM AZM (E) on FPDc during 7-day treatment and following 7-day washout. iPSC-CMs derived from four donors were used for MEA recording. For the initial recording (day 0), $10 \leq n \leq 13$ for all conditions. Spontaneous beating status of iPSC-CMs is listed in Supplementary Table 1. Two-way ANOVA with Bonferroni post-hoc test was used for statistical evaluation (* $p < 0.05$, ** $p < 0.01$, *** $p < 0.001$ and **** $p < 0.0001$).

HCQ and AZM independently and synergistically augment the conduction velocity of iPSC-CMs

Since conduction disorders were the most frequent side effect that appeared in COVID-19 patients who were administrated with HCQ and AZM[6], we examined the impact of the two drugs on cardiac conduction velocity (CV) in iPSC-CM model. As shown in Figure 5, CV of iPSC-CMs in the control group remained stable during the two-week experiment. While cells treated with 1 µM AZM showed a similar conduction trajectory and CV as in the control group, 10 µM AZM led to changes in trajectory and significantly augmented CV in iPSC-CMs, starting on day 3 after drug treatment, but reversing on day 3 after drug washout (Figure 5A and B). Similar to AZM, HCQ also resulted in changes in conduction trajectory and increases in the CV of iPSC-CMs in a concentration-dependent pattern (Figure 5A and C). The addition of 1 µM AZM enhanced the effects caused by HCQ alone (Figure 5D). Furthermore, when 10 µM AZM was applied in addition to HCQ (1, 3, and 10 µM), iPSC-CMs from all three groups showed significantly faster transmission of electrical signals (Figure 5A and E).

Figure 5

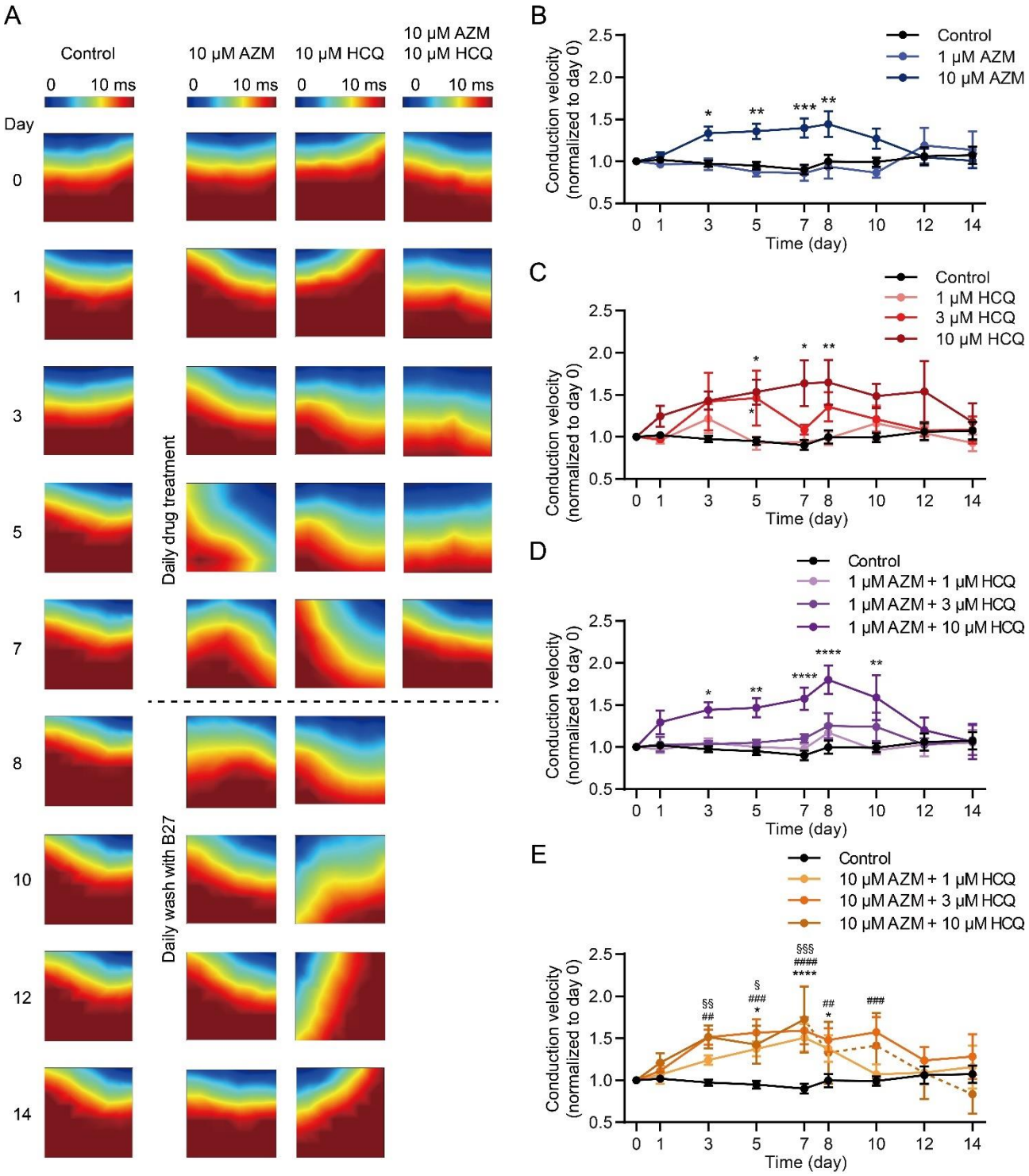

Figure 5: Changes in conduction trajectory and augmented CV in iPSC-CMs treated with AZM and HCQ alone and in combination. A, Representative heatmaps illustrating the conduction trajectories of electrical signals in iPSC-CMs under different conditions during 7-day drug treatment and following 7-day washout. Due to cell death, no signal was captured in cells treated with 10 μM HCQ and 10 μM AZM in combination in the washout period. B, C, CV of iPSC-CMs treated with AZM (B) and HCQ (C) for 7 days and following washout for 7 days (normalized to day 0). D, E, CV

of iPSC-CMs treated with 1 µM AZM (D) and 10 µM (E) combined with HCQ (1, 3, and 10 µM) during 7-day treatment and following 7-day washout. iPSC-CMs derived from four donors were used for MEA recording. For the initial recording (day 0), $10 \leq n \leq 13$ wells for all conditions. Spontaneous beating status of iPSC-CMs is listed in Supplementary Table 1. Two-way ANOVA with Bonferroni post-hoc test was used (* $p < 0.05$, ** $p < 0.01$, *** $p < 0.001$, and **** $p<0.0001$).

HCQ and AZM synergistically enhance the expression of Cx43 and alter the steady-state kinetics of I_{Na} in iPSC-CMs

To gain insights into the molecular mechanism of HCQ/AZM-induced CV augmentation, we analyzed expression of Nav1.5 and Cx43, which are crucial to maintain electrical signal propagation between CMs[24]. Compared to the control group, the expression of Nav1.5 was slightly, but not significantly, higher in iPSC-CMs treated with 10 µM HCQ for 7 days ($p > 0.05$, Figure 6A, B). Treatment with 10 µM AZM did not change Nav1.5 protein levels ($p > 0.05$, Figure 6A, B). Importantly, when we applied 10 µM HCQ combined with 10 µM AZM to iPSC-CMs, we observed a 2-fold increase in Nav1.5 protein expression ($p > 0.05$, Figure 6A, B). In terms of Cx43, 7-day treatment with 10 µM HCQ significantly increased the protein expression by 3-fold ($p < 0.01$, Figure 6A, C). While treatment with 10 µM AZM alone only slightly increased the Cx43 expression ($p > 0.05$), the combination of 10 µM HCQ and 10 µM AZM synergistically quadrupled the expression of Cx43 compared to the control group (Figure 6A, C). Similar results were observed using immunofluorescence staining, revealing a higher expression as well as a strong intracellular accumulation of Cx43 in iPSC-CMs treated with 10 µM HCQ, 10 µM AZM, and their combination (Figure 6D).

To further investigate the impact of HCQ and AZM on the function of cardiac sodium channel, we recorded I_{Na} in cells treated with 10 µM HCQ and/or 10 µM AZM for 7 days using an automated patch-clamp technique (Supplementary Figure 7). Compared to the control group, iPSC-CMs treated with 10 µM AZM alone showed increased membrane capacitances (an indicator for cell size), while cells treated with 10 µM HCQ in combination with 10 µM AZM showed lower membrane capacitances (Supplementary Figure 7B). We could not observe differences regarding the current density of I_{Na} in the four groups, except that the reversed current at +70 mV was smaller in cells treated with combined HCQ and AZM (Supplementary Figure 7A, C). However, both drugs markedly modified the gating properties of cardiac sodium channel. Compared to the control group, the steady-state activation curves were leftwards shifted in the groups treated with HCQ alone or in combination with AZM, but not in iPSC-CMs treated with AZM alone (Supplementary Figure 7D). Moreover, the steady-state inactivation curves of all the three groups treated with the drugs showed a rightwards shift (Supplementary Figure 7E).

Figure 6

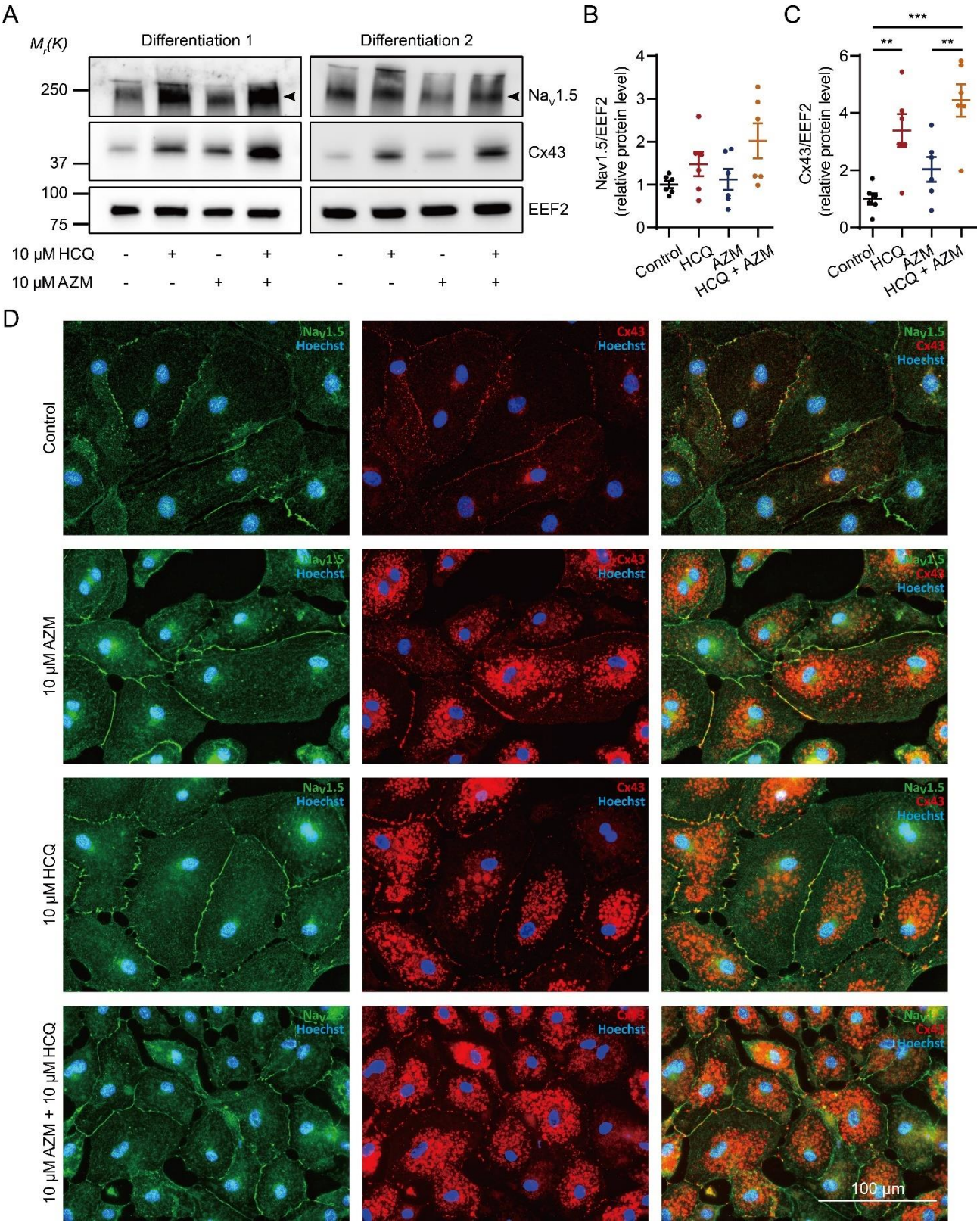

Figure 6: Nav1.5 and Cx43 protein expression in iPSC-CMs treated with HCQ and/or AZM. A, Two representative western blots showing the expression of Nav1.5 and Cx43 in iPSC-CMs under different drug treatment conditions. B, Quantitation of protein expression levels of Nav1.5 in iPSC-CMs under different conditions; N = 6 independent differentiations. C, Quantitation of protein

expression of Cx43 in iPSC-CMs under different drug treatment conditions; N = 6 independent differentiations. D, Representative images showing immunostaining for Nav1.5 (green) and Cx43 (red) in iPSC-CMs under different drug treatment conditions. Cell nuclei are shown in blue (Hoechst). Statistical evaluation was performed using one-way ANOVA with Tukey's multiple comparison test (** $p < 0.01$, and *** $p < 0.001$).

HCQ and AZM accumulate in iPSC-CMs

As HCQ and AZM have been reported to accumulate in lysosomes and endosomes, we analyzed the levels of HCQ and AZM in lysates of iPSC-CMs after 7-day drug treatment using mass spectrometry. Due to reduced cell viability in combination treatments with higher concentrations of HCQ and AZM, we did not include these groups in the analysis. Our data reveal that cellular levels of HCQ (Figure 7A) and AZM (Figure 7B) increased in a concentration-dependent manner after the 7-day treatment. Interestingly, levels of HCQ in iPSC-CMs treated with 1 µM HCQ combined with 10 µM AZM were much higher than those in cells treated with 1 µM HCQ alone (Figure 7A) and accumulation of AZM was increased by co-treatment with 1 µM or 3 µM HCQ (Figure 7B). These data indicate that the combined treatments with HCQ and AZM facilitate cellular accumulation of HCQ and AZM and provide further evidence for the synergistic effects of AZM and HCQ through increased cellular accumulation.

Figure 7

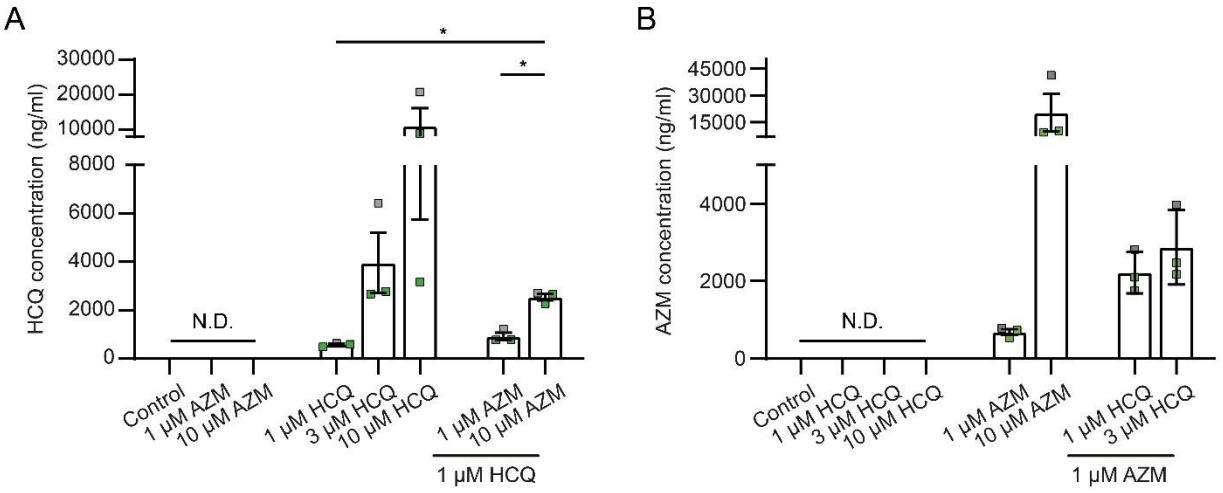

Figure 7: Accumulation of HCQ and AZM in iPSC-CMs after 7-day treatment. A, B, Concentrations of HCQ (A) and AZM (B) in cell lysates from iPSC-CMs after the 7-day treatment with HCQ and AZM at different conditions, determined using mass spectrometry. Data represent mean and SEM of N = 3 independent experiments, performed with iPSC-CMs from 2 healthy donors (iBM76.1, iBM76.3 in green; iWTD2.1 in grey). N. D., below detection limit. Statistical evaluation was performed using one-way ANOVA with Tukey's multiple comparison test (* $p < 0.05$).

Discussion

The combination therapy with HCQ and AZM was initially reported to reduce viral load and to improve disease progression of COVID-19 patients[2], which could not be confirmed in follow-up studies[4, 25]. In contrast, HCQ/AZM combination therapy was associated with increased cardiac complication rates in comparison to monotherapy with HCQ or AZM[17]. In this study, we examined the effects of HCQ and AZM on iPSC-CM structure and function for a period of 7 days, similar to clinical treatment durations of 5 – 10 days[2, 4, 18, 25, 26]. Drug concentrations ranging from 1 to 10 µM were defined based on the antiviral potency of HCQ (EC_{50}: 4.2 µM) and AZM (EC_{50}: 2.1 µM)[27] and the reported dosages used for COVID-19 patients (600 – 800 mg/day for HCQ and 250 – 500 mg/day for AZM). The therapeutic blood levels of HCQ for systemic lupus erythematosus was 1.5 µM to 6 µM in patients receiving a dose of 200 or 400 mg/day[28, 29]. Although AZM plasma level was rather low, ~ 0.3 µM in patients receiving a dose of 250 mg daily[30, 31], AZM is known to accumulate rapidly in cells[31, 32, 33, 34, 35, 36].

As MEA-measurements and video-based motion analysis allow frequent documentation of iPSC-CM function during 7 days of drug treatment, our study provides first evidence for the functional consequences of AZM and HCQ under long-term treatment, whereas insights from previous studies are limited to acute or short-term treatment[16]. We show that both AZM and HCQ negatively affect the viability, morphology, sarcomeric structure as well as the contractile and electrophysiological function of iPSC-CMs at clinically relevant concentrations and treatment duration. Interestingly, the combination with AZM strongly increased HCQ-induced reduction of cell viability as well as changes in contractile and electrophysiological function. Moreover, we demonstrate that HCQ and AZM increased Cx43 and Nav1.5 protein levels in a synergistic manner, which may underlie the severe electrophysiological dysfunction. Mechanistic insights on the synergistic effect of HCQ and AZM are provided by the increased accumulation of the drugs in iPSC-CMs when applied in combination.

HCQ and AZM differentially affect iPSC-CM viability and functionality

In this study, treatments with AZM and HCQ alone revealed that both drugs at higher concentrations negatively impact cell viability, morphology, sarcomeric structure, the contractility, and electrophysiological function of iPSC-CMs. At an equimolar concentration of 10 µM, however, a significantly higher cardiotoxic activity of HCQ than that of AZM was observed, as shown by lower MTT reduction to formazan, lower cell density and higher LDH activity after the 7-day treatment (Figure 1). Even after 7 days of drug washout, a progressive cardiotoxic effect of HCQ was detected not only by the MTT assay, morphological analysis, but also by the increasing number of iPSC-CM cultures which stopped spontaneous beating (Supplementary Table 1).

Besides the reduced cell viability, treatment with 10 µM HCQ resulted in a progressive increase in FPDc, CV and beating frequency in iPSC-CMs during the 7-day treatment. The increased FPDc was also reported in the guinea pig heart upon acute treatment with 10 µM HCQ alone *ex vivo*[16]. In our study, we observed a slight reduction of FPDc in iPSC-CMs after the 7-day treatment with 10 µM AZM alone, while CV was increased to a similar extend as in cells treated with 10 µM HCQ. Interestingly, AZM led to an initial increase in the beating frequency on day 1, but a decrease to control levels on day 3 and a further decrease until day 7. The AZM-induced increase in the beating rate at day 1 is in line with the previous study showing that treatment of HL-1 CMs with 100 µM AZM for 24 hours dramatically increased the spontaneous beating frequency[31]. Although several studies reported the electrophysiological effects of HCQ or AZM in cardiomyocytes *in vitro*, our study is the first to evaluate HCQ and AZM in terms of the effect of clinically relevant long-term treatment[31].

In agreement with the reduced cell viability and impaired electrophysiological function, iPSC-CMs also showed altered contractile performance. Treatment with 10 µM AZM or HCQ led to decreased contraction and relaxation time as well as highly varying contraction and relaxation velocities, indicating that treatments with AZM or HCQ at a high concentration over a long time period interfere with the ability of iPSC-CMs to contract in a coordinated manner. In a recent publication, the effects of two cardiotoxic drugs, doxorubicin (DOX) and trastuzumab (TRZ), on the viability and function of iPSC-CMs were reported[37]. Unlike in our study, spontaneous beating frequency and electrical propagation of iPSC-CMs were not affected by DOX and TRZ, but the contraction velocity and displacement (or deformation distance) were reduced. These findings point towards different mechanisms of drug-induced cardiac complications induced by AZM and HCQ compared to DOX and TRZ. The adverse effects induced by DOX and TRZ were proposed to be linked to drug-induced mitochondrial dysfunction and altered cardiac energy metabolism[37]. Based on our results, we assume that the HCQ-induced increase in CV and alteration in contraction may be caused by enhanced expression (or accumulation) of Cx43 and altered gating properties of the sodium channel[37]. Acute treatment with HCQ was reported to have an effect on I_{Na} with an IC_{50} of 113.9 ± 78.3 µM, which may explain the reduction in the electrical signal transmission observed in the guinea pig heart treated with 10 µM HCQ *ex vivo*[16]. In our study, we observed no effect of 10 µM HCQ on I_{Na} after the 7-day treatment, but altered gating properties. This may account for the different effect of HCQ on CV in iPSC-CMs compared to that in the whole heart after acute treatment with 10 µM HCQ. In addition, we cannot exclude the possibilities that these different effects are due to species differences between humans and guinea pigs.

It is worth mentioning that the effects of AZM and HCQ at low concentrations (1 or 3 µM) on cell area, and sarcomere structure of iPSC-CMs were relatively mild but failed to recover to the control level after 7 days of drug washout, suggesting that AZM and HCQ may induce persistent, long-

term damage of iPSC-CM structure. In addition, treatment with AZM caused cellular hypertrophy, as shown by increased cell area and higher membrane capacitance (Figure 2B, Supplementary Figure 7B) whereas HCQ (1 or 3 µM) resulted in the reduced cell area in a concentration-dependent pattern.

Overall, investigation of the individual effects of AZM and HCQ on iPSC-CMs revealed remarkable differences in their influence on the beating frequency, contractile properties as well as FPDc.

Synergic effects between AZM and HCQ

Higher mortality rates, significantly increased risks for cardiac arrest[15], and greater QTc prolongation[18, 19] were observed in patients treated with HCQ and AZM in combination compared to treatment with either HCQ or AZM. By treating iPSC-CMs with a combination of AZM and HCQ, we confirmed this synergistic effect, which caused a strong reduction in cell viability, sarcomere disorganization, conduction abnormalities and contractile dysfunction.

Although treatment with 10 µM AZM had no effect on cell viability, the combination of 10 µM HCQ with 1 µM or 10 µM AZM significantly enhanced the cytotoxicity of 10 µM HCQ, as indicated by lower MTT reduction to formazan and increased LDH activity. This potential of AZM to enhance cytotoxic effects of different drugs was previously demonstrated in cancer cell lines for the combination of AZM with Lansoprazol[38] or gefitinib[39].

Similar to the viability studies, the combination of AZM with HCQ led to the most pronounced reductions in cell area, sarcomere length and degree of sarcomeric organization, compared to the effects of AZM or HCQ alone[40]. In autopsy samples of COVID-19 patients regardless of the presence of clinical cardiac manifestations or myocarditis, infection of myocardium with SARS-CoV-2 was confirmed in 60% of patients[40] and CM necrosis, and myofibrillar anomalies were reported[41, 42]. These findings could be recapitulated using iPSC-CMs infected with SARS-CoV-2[41, 42]. However, no data on cytopathic features in the heart of COVID-19 patients with HCQ and AZM treatment are available. Considering the strong effect of HCQ combined with AZM on iPSC-CMs on viability and sarcomeric structure demonstrated in our study, this may explain the increased rate of cardiac complications with this combination treatment. It is of great interest to study whether the treatment of COVID-19 patients with HCQ and AZM could worsen cell viability and cardiac structural abnormalities in the heart autopsies.

Furthermore, the changes in contractile function and electrophysiological properties were more pronounced in iPSC-CMs treated with AZM and HCQ in combination. In the presence of 10 µM AZM, the changes in contraction and relaxation time were already enhanced in combination with 1 µM HCQ and were even more pronounced with 3 µM and 10 µM HCQ. In addition, the HCQ-induced prolongation of FPDc and increase in CV were further exacerbated in the presence of 10

μM AZM. Of note, documentations of the iPSC-CMs during the 7-day washout period revealed reversibility of the changes in FPDc and CV in some cultures. However, more iPSC-CM cultures with AZM and HCQ combination treatment showed beating arrest compared to treatment with HCQ and AZM alone. These results demonstrate that the application of AZM together with HCQ worsens the adverse effects of HCQ to induce contractile and electrophysiological dysfunction in iPSC-CMs. These data are in line with the increased expression of Nav1.5 and Cx43 in iPSC-CMs, which are induced by HCQ and AZM in a synergistic manner. However, it is difficult to speculate whether these functional changes can recapitulate the heart functionality in COVID-19 patients because a plethora of other factors are involved in affecting cardiac functionality. Mimicking the cytokine storm in patients with severe COVID-19, a recent study demonstrated that treatment of cardiac microtissue derived from iPSC-CMs with a cocktail of interleukin 1β, interferon-γ and polyinosinic:polycytidylic acid exhibited an increase in contractile force as well as prolongation of contraction and relaxation time[43].

Mechanistic evidence of AZM and HCQ combination

HCQ and AZM are lysosomotropic compounds known to accumulate in lysosomes and to increase lysosomal pH, which is critical for the inhibition of viral infection[44]. Determination of drug levels in iPSC-CMs after the 7-day treatment with AZM or HCQ alone revealed that the cellular levels correlated with the drug concentrations used. Interestingly, cellular levels of AZM were higher when HCQ was present and vice versa, indicating that the combined treatment favors the accumulation of both compounds in iPSC-CMs. Previous study suggested that the ATP-dependent translocase ABCB1 played an important role in the synergistic effects of AZM and HCQ. ABCB1 is located in the cell membrane and lysosomal membrane, acts as an AZM-transporter and is known to be inhibited by HCQ[45]. However, involvement of ABCB1 in the synergistic effect of AZM and HCQ in iPSC-CMs is unlikely, as RNA-sequencing data from our group as well others reveal that ABCB1 is not expressed in iPSC-CMs[46, 47]. So far, the mechanism for the increased cellular accumulation of AZM and HCQ with combined treatment is unclear.

Activation of integrated stress response (ISR) pathway and inhibition of autophagosome formation by AZM and HCQ likely explain the strong intracellular accumulation of Nav1.5 and Cx43. Previous studies showed that application of CQ increased the abundance of Cx43 in neonatal rat ventricular myocytes through its lysosomal inhibiting ability and prolongation of Cx43 turnover[48, 49]. Remarkably, our study shows that the synergistic effect of AZM and HCQ increased Cx43 expression by 4-fold, which was significantly higher than the increase in Cx43 protein expression observed by treatment with AZM alone. Additionally, 7-day treatment with AZM and HCQ increased protein expression of Nav1.5 but did not increase sodium current density, suggesting

that the availability of functional sodium channels on the membrane was not altered despite the intracellular accumulation[31]. As cardiac conduction is determined not only by sodium channel availability but also by gap junction expression and function, our data suggest that the significantly increased expression of the gap junctional protein Cx43 may contribute to the increased CV in iPSC-CMs after 7-day treatment with HCQ or HCQ and AZM in combination.

Taken together, our results reveal that the more severe effects of the combined treatment with AZM and HCQ on viability, structure and functionality of iPSC-CMs may be caused by an increased intracellular accumulation of the drugs. The synergistic upregulation of Cx43 protein levels by AZM and HCQ provide first mechanistic evidence for the increased cardiac complications observed with the combination treatment.

Study limitations

Aiming to gain mechanistic insights for the increased rates of cardiac complications observed for the combined treatment with AZM and HCQ, we characterized the consequences of the two drugs as well as their combination on the viability, structure and functionality of iPSC-CMs. Despite iPSC-CMs represent an important model system to study drug effects on the human heart, different aspects, including the immaturity of the cells and the lack of the multicellular environment limit, the predictive value of our findings. Furthermore, modeling the situation in patients with severe COVID-19 may require infection of iPSC-CMs with SARS-CoV-2 before drug treatment to model structural and functional abnormalities, which will make the execution of the study technically challenging.

Conclusions

Through the systematic investigation of the effects of AZM and HCQ individually as well as in combination, we show that these two drugs had adverse effects on the viability, structure and functionality of human cardiomyocytes. These adverse effects get more severe when AZM and HCQ are applied in combination, thus recapitulating the higher rates of cardiac complications observed with the AZM/HCQ combination treatment in clinical use. This synergistic activity of AZM and HCQ in iPSC-CMs is likely driven by the increased intracellular accumulation of the drugs when applied in combination. Furthermore, we provide evidence that the HCQ-induced increase in conduction velocity is caused by elevated levels of Cx43, which further increase in combination with AZM.

Materials and Methods

Culture and maintenance of iPSCs

Human iPSC lines used in this study were reprogrammed from somatic cells of four healthy individuals. The cell lines iWTD2.1/2.3 (UMGi001-A clone 1 and clone 3) and iBM76.1/76.3 (UMGi005-A clone 1 and clone 3) were generated from dermal fibroblasts and mesenchymal stem cells, respectively, using STEMCCA lentivirus, and characterized as previously described[46, 50]. The cell lines isWT1.13 (UMGi014-C clone 3) and isWT7.22 (UMGi020-B clone 22) were generated from dermal fibroblasts using the integration-free CytoTune-iPS 2.0 Sendai Reprogramming Kit (Thermo Fisher Scientific), and characterized previously[51]. The iPSC generation was approved by the Ethics Committee of the University Medical Center Göttingen (approval number: 21/1/11 and 10/9/15) and used following the approval guidelines. To maintain the growth of iPSCs, a chemically defined E8 medium (Thermo Fisher Scientific) was used, and cells were cultivated on Geltrex (Thermo Fisher Scientific) coated plates at 37°C with 5% CO_2. The E8 medium was changed on a daily basis and cells at ~85% confluency were passaged using Versene (Thermo Fisher Scientific).

Differentiation of iPSCs into cardiomyocytes and drug treatment

Directed differentiation of iPSCs into cardiomyocytes was induced by modulating the WNT signaling cascade as described[52, 53]. In brief, when iPSCs grown on 12-well plates reached 80~90% confluency, the medium was changed from the E8 medium to cardio differentiation medium, which composed of RPMI 1640 with Glutamax and HEPES (Thermo Fisher Scientific), 0.5 mg/ml human recombinant albumin (Sigma-Aldrich) and 0.2 mg/ml L-ascorbic acid 2-phosphate (Sigma-Aldrich). To initiate differentiation, cells were incubated with 4 µM CHIR99021 (a GSK3β inhibitor, Millipore) for 48 hours followed by incubation with 5 µM IWP2 (a WNT signaling inhibitor, Millipore) for additional 48 hours. Thereafter, cells were kept in cardio differentiation medium for four days with medium change every second day. The first beating cells were detected on day 8 post differentiation. From day 8, cells were cultivated in RPMI/B27 medium containing RPMI 1640 with Glutamax and HEPES, supplemented with 2% B27 (Thermo Fisher Scientific).

To maintain a long-term culture, iPSC-CMs were replated from 12-well plates into 6-well plates at day 20 post differentiation. Briefly, cells were incubated with 1 mg/ml collagenase B (Worthington Biochemical) for 1 hour at 37°C. Detached iPSC-CM clusters were gently collected into a 15 ml Falcon tube and dissociated with 0.25% trypsin/EDTA (Thermo Fisher Scientific) for 8 min at 37°C. Dissociated iPSC-CMs were resuspended in cardio digestion medium (80% RPMI/B27 medium, 20% fetal calf serum, and 2 µM thiazovivin) and cultured in Geltrex-coated 6-well plates at a density of 800,000 cells per well for 24 hours. Afterward, iPSC-CMs were cultivated in RPMI/B27 medium.

To perform functional analyses, 70-day-old iPSC-CMs were dissociated again with collagenase B

and trypsin stepwise, and replated for different assays. One week after replating, the cells were treated with HCQ and AZM alone or in combination at different concentrations for 7 days, with daily medium change, followed by a 7-day washout period with RPMI/B27 medium (Supplementary Figure 1). HCQ (EMD Millipore) was dissolved in ddH_2O and AZM (Sigma-Aldrich) was dissolved in DMSO to prepare 10 mM stock solutions, which were aliquoted and stored at -20°C.

Video-based contraction analysis

Video-based analyses were used to examine drug effects on the contractile parameters of iPSC-CMs. To this end, iPSC-CMs were replated into Geltrex-coated 48-well plates at a density of 60,000 cells per well one week before drug treatment. Videos were obtained using an ORCA Flash 4.0 V3 CMOS camera (Hamamatsu, 60 FPS, 1024x1024 pixels resolution) on days 0 (before treatment), 1, 3, 5, and 7 of the treatment-period. Video data were analyzed using the cellular motion analysis software *"Maia"* (QuoData – Quality & Statistics GmbH) to evaluate the beating properties[54]. Analysis settings were: block size 20.3 µm (16 pixels), frameshift 100 ms, and maximum distance shift 8.9 µm (7 pixels). For every condition, videos were obtained from 3 different wells with two videos on different areas of each well. For analysis, data were normalized to control without drugs of the respective day.

Immunofluorescence staining

For immunostainings, iPSC-CMs were seeded into Geltrex-coated 12-well or 6-well plates prepared with coverslips at a density of 15,000 or 200,000 cells per well, respectively. After seeding, cells were cultured for 7 days in RPMI/B27 medium before drug treatment. On day 7 (after drug treatment for 7 days) or day 14 (after drug washout for 7 days), cells were washed 2 times for 5 minutes in relaxation buffer (PBS supplemented with 5 mM EGTA and 5 mM $MgCl_2$), followed by 2 times wash with PBS and fixation in ice-cold methanol-acetone (7:3, *v/v*) solution for 20 minutes at -20°C. Fixed cells were washed 3 times for 5 minutes with PBS, followed by blocking in 1% BSA for at least 2 hours at 4°C. For staining, cells were incubated with the following primary antibodies: anti-α-actinin, clone EA-53 (1:500; mouse monoclonal, IgG1, Sigma-Aldrich, 7811), anti-Nav1.5 (1:200; rabbit polyclonal, Alomone Labs, ASC-005), and anti-Cx43, clone 2 (1:1000; mouse monoclonal, IgG1, BD Biosciences, 610061) at 4°C overnight. Afterward, cells were washed three times with PBS and incubated with the corresponding secondary antibodies (1:1000; anti-rabbit Alexa Fluor 488, Invitrogen, A11008; anti-mouse Alexa Fluor 488, Invitrogen, A11001; or anti-mouse Alexa Fluor 546, Invitrogen, A11030) for 1 hour at room temperature. Cell nuclei were counterstained with Hoechst33342 (1:1000; Thermo Fisher Scientific) in PBS for 20 minutes. Coverslips were mounted on glass slides using Fluoromount-G mounting medium (Thermo Fisher Scientific). Stained iPSC-CMs were imaged using a fluorescence microscope (Keyence BZ-X700E). The exposure time was calibrated based on staining controls performed using only

secondary antibody. Quantification of cell area was performed based on α-actinin stained iPSC-CMs using Cell Profiler[55] and manual analysis with FIJI[56]. Sarcomere-length was determined manually using FIJI as described previously[22]. The amount of structurally organized iPSC-CMs with evenly distributed intact sarcomeres across the cell body (occupying > 80% of the cell area) and disorganized cells was determined using manual counting.

Multi-electrode array

For FP measurement, iPSC-CMs were seeded in the cavity containing electrodes of the Geltrex-coated CytoView 6-well MEA plates (Axion BioSystems). Around 300,000 iPSC-CMs were first resuspended in 20 µl cardio digestion medium and seeded in the electrode-containing cavity of the MEA plates. One hour later, an additional 1 ml of medium was added into each well, and iPSC-CMs were kept in RPMI/B27 medium for one week before drug treatment. For every batch of experiment, at least two wells of iPSC-CMs from different plates were treated with the same condition to avoid plate variability. Spontaneous FP recordings were carried out using the Maestro Edge equipped with AxIS Navigator software (Axion BioSystems) with a sample rate of 12,500 Hz at 37°C with 5% CO_2. From day 0 (the day before treatment) to day 14 (last day for washout), FPs were recorded daily for all conditions used (Supplementary Figure 1). Several key parameters including conduction velocity (CV), corrected FPD_C (corrected by Fridericia's formula) and inter-beat interval were determined using AxIS Navigator, and further analyzed with AxIS Metric Plotting Tool (Axion BioSystems). Spontaneous beating frequency was defined as the reciprocal of averaged inter-beat interval. The mainstream CV values were averaged for one culture.

Automated patch-clamp

To investigate the effect of high concentration of HCQ and AZM on the function of sodium channel, the properties of I_{Na} were examined in iPSC-CMs treated with 10 µM HCQ alone, 10 µM AZM alone or their combination, respectively. The drug treatment lasted for 7 days with daily medium change, and iPSC-CMs kept in RPMI/B27 medium served as control. Recording of I_{Na} was performed using the Patchliner Quattro (Nanion Technologies GmbH) with low resistance NPC-16 chips at room temperature as described previously[52, 57]. In brief, iPSC-CMs were dissociated gently into single cells. Capture of single cells and formation of whole-cell configuration were processed automatically by Patchliner. From a holding potential of -100 mV, I_{Na} was recorded under pulses ranging from -90 to +70 mV for 20 ms in 5 mV increment with an interval of 2 s. Currents were sampled at 25 kHz and low-pass-filtered at 2.9 kHz.

Western Blot

Three-month-old iPSC-CMs were treated with 10 µM HCQ, or 10 µM AZM, or the combination of HCQ and AZM for seven days, snap-frozen in liquid nitrogen and stored at -80°C. To detect the expression of specific proteins, cells were lysed by homogenization in RIPA buffer (150 mM NaCl,

50 mM Tris, 1.0% NP-40, 0.5% sodium deoxycholate, 0.1% SDS, 1 mM EDTA, 10 mM NaF, and 1 mM PMSF), supplemented with protease (cOmplete mini, EDTA-free) and phosphatase (PhosSTOP) inhibitors and incubated for 30 min at 4°C with gentle rotation. Cell homogenates were clarified by centrifugation at 14,000 rpm for 20 min at 4°C and protein concentration was measured using a BCA assay following the manufacturer's instruction. 30 µg of proteins were subjected to SDS-PAGE using a 4-15% gradient gel (BioRad) and transferred onto nitrocellulose membranes. Membranes were blocked in 5% milk in TBS-T for 30-45 min at room temperature and probed with anti-Cx43, clone 4E6.2 (1:1000; mouse monoclonal, Merck, MAB3067), anti-Nav1.5 (1:200; rabbit polyclonal, Alomone Labs, ASC-005), or anti-EEF2 (1:5000; rabbit polyclonal, Abcam, ab40812) at 4°C overnight, followed by incubation with horseradish peroxidase-conjugated secondary antibodies goat anti-mouse (1:10,000; Sigma Aldrich, A2304) or goat anti-rabbit (1:10,000; Cell Signaling, 7074S), respectively, for 1 hour at room temperature. Proteins were visualized by chemiluminescence using the Super Signal West Dura Chemiluminescent Substrate kit in combination with the Fusion FX Spectra Imaging System (Peqlab). Densitometry analyses of the immunoblots were performed using ImageJ software and the intensity of individual bands was normalized to EEF2.

Lactate dehydrogenase measurement

Measurement of LDH activity was performed using LDH assay kit (Abcam, ab102526) according to the manufacturer's instructions in supernatants of iPSC-CM cultures after 7 days of drug treatment and after subsequent 7 days of drug washout. Briefly, 50 µl of cell supernatant was mixed with 50 µl substrate solution in a 96 well plate. Absorption was measured at 450 nm in a kinetic mode, every 2 minutes for 60 minutes (Biotek Synergy HTX). LDH activity was calculated based on a standard curve according to the manufacturer's instructions (equation 1).

Equation 1: Calculation of LDH activity

$$LDH\ activity\ \left[\frac{mU}{ml}\right] = \left(\frac{Amount\ of\ NADH\ in\ sample\ calc.\ from\ standard\ curve[nmol]}{reaction\ time\ [min]\ \mathrm{x}\ Sample\ volume\ [ml]}\right) * Dilution\ factor$$

MTT assay

Cell viability was determined using MTT assay kit (Millipore, CT02) according to the manufacturer's instructions. After drug treatment as well as after drug washout, cells were washed twice with pre-warmed PBS and incubated in 200 µl RPMI/B27 medium per well with 0.5 mg/ml MTT for 2 hours at 37°C. Subsequently, 300 µl of isopropanol with 0.04 N HCl was added and samples were mixed thoroughly by pipetting to facilitate cell lysis and the dissolving of formazan. Absorbance was measured at 570 nm (formazan) and 630 nm (reference) using plate reader (Biotek Synergy HTX). Viability was calculated as $A_{570} - A_{630}$.

Determination of HCQ and AZM concentration in cell lysates

Intracellular drug accumulation was determined from cell lysates of the MTT assay using mass spectrometry. After MTT measurement, cell lysates were stored at -20°C for 1-4 days prior to detection. The stability of HCQ and AZM under these conditions was confirmed for up to 7 days at -20°C. 25 µl fresh or thawed cell lysates were diluted with 225 µl 2 mM ammonium acetate buffer, vortexed and centrifuged for 10 minutes (14,000 rpm). 10 µl of the clear supernatants were injected into the LC-MS/MS, which consists of an UltiMate3000 pump, an autosampler (Dionex, ThermoScientific) and an API 4000 Tandem mass spectrometer (ABSciex) using positive Electrospray Ionization (ESI+ ; 4500 V). HCQ and AZM were determined by a Synergi 4µ HydroRP 80A column 150 mm x 3.0 mm (Phenomenex, Aschaffenburg, Germany) using a binary gradient with 2 mM ammonium acetate buffer and acetonitrile and a flow rate of 0.5 ml/min. The resulting retention times were 3.0 min for HCQ and 3.2 min for AZM. HCQ and AZM were measured using the multiple reaction monitoring mode (MRM) with nitrogen as collision gas. The method was suitable for the quantification of HCQ and AZM in cell lysates over the range from 20 to 1000 ng/ml. Samples with higher concentration were diluted.

Statistics

Results about cell area are presented as median ± 95% CI and results for the other parameters are presented as mean ± standard error of the mean (SEM). Statistical analysis was performed with GraphPad Prism 9. One-way ANOVA with Tukey's multiple comparison was used for cell viability, cell area, sarcomere length, contractility property, protein expression level, and drug accumulation data. Two-way ANOVA with Bonferroni post-hoc test was used for MEA assay-based FPDc, CV and beating rate data, as well as Patchliner assay-based I_{Na} data. p-value < 0.05 was considered statistically significant.

Acknowledgments

We thank Jessie Pöche, Konstanze Fischer, Ying Ulbricht, Julian Leefmann and Judith Müller (Dresden) and the entire team from the Stem Cell Unit (Göttingen) for their excellent technical assistance.

Authors contribution statement

Study conceptualization by WL, XL, MSchu, KG, KN, and SU. Supervision was performed by SU and KG, and project administration by MSchu, KG, KH, SU and KS. WL. XL, MSP, AS, RO, LC and MSchu conducted investigation, and WL, XL, MSP, AS, RO, KN, MH, R-PS, MSchu, and KG performed data curation and formal analysis. WL, XL, KH, SU, MSchu, and KG contributed to the validation and interpretation of the data. Software was developed by KN, MS, KH, and SU. KG and KS acquired funding, and KG, SU and KS provided resources. The original draft was prepared by

711 WL, XL, RO, MSP, MSchu, and KG, and reviewed/edited by LC, KN, and SU.

712 ## Funding

713 The work was supported by the Free State of Saxony and the European Union EFRE (SAB
714 projects “PhänoKard” and “PhenoCor” to K. Guan as well as “HERMES” to QuoData – Quality &
715 Statistics GmbH (K. Simon and S. Uhlig) and K. Guan), by the German Federal Ministry of
716 Education and Research/German Center for Cardiovascular Research (to L. Cyganek), and by the
717 German Research Foundation (Project Number 193793266 – SFB1002 S01, to L. Cyganek). M.
718 Schubert was supported by the MeDDrive START grant from the Medical Faculty at TU Dresden.
719 A. Strano and M. Hasse were financially supported by the Deutsche Forschungsgemeinschaft
720 (DFG, German Research Foundation) – Project Number 288034826 – IRTG 2251: “Immunological
721 and Cellular Strategies in Metabolic Disease”.

722 ## Disclosures

723 The authors declare that they have no known competing financial interests or personal
724 relationships that could have appeared to influence the work reported in this paper.

725

References

1. Dixit SB*, et al.* Current Approaches to COVID-19: Therapy and Prevention. *Indian J Crit Care Med* **24**, 838-846 (2020).

2. Gautret P*, et al.* Hydroxychloroquine and azithromycin as a treatment of COVID-19: results of an open-label non-randomized clinical trial. *Int J Antimicrob Agents* **56**, 105949 (2020).

3. Andreani J*, et al.* In vitro testing of combined hydroxychloroquine and azithromycin on SARS-CoV-2 shows synergistic effect. *Microbial Pathogenesis* **145**, 104228 (2020).

4. Furtado RHM*, et al.* Azithromycin in addition to standard of care versus standard of care alone in the treatment of patients admitted to the hospital with severe COVID-19 in Brazil (COALITION II): a randomised clinical trial. *Lancet* **396**, 959-967 (2020).

5. Geleris J*, et al.* Observational Study of Hydroxychloroquine in Hospitalized Patients with Covid-19. *N Engl J Med* **382**, 2411-2418 (2020).

6. Lane JCE*, et al.* Safety of hydroxychloroquine, alone and in combination with azithromycin, in light of rapid wide-spread use for COVID-19: a multinational, network cohort and self-controlled case series study. *medRxiv*, 2020.2004.2008.20054551 (2020).

7. Lane JCE*, et al.* Risk of hydroxychloroquine alone and in combination with azithromycin in the treatment of rheumatoid arthritis: a multinational, retrospective study. *The Lancet Rheumatology*, (2020).

8. Li C, Cheng G. Will Hydroxychloroquine Still Be a Game-Changer for COVID-19 by Combining Azithromycin? *Frontiers in Immunology* **11**, (2020).

9. Chatre C, Roubille F, Vernhet H, Jorgensen C, Pers Y-M. Cardiac Complications Attributed to Chloroquine and Hydroxychloroquine: A Systematic Review of the Literature. *Drug Safety* **41**, 919-931 (2018).

10. Roden DM, Harrington RA, Poppas A, Russo AM. Considerations for Drug Interactions on QTc in Exploratory COVID-19 Treatment. *Circulation* **141**, e906-e907 (2020).

11. Capel RA*, et al.* Hydroxychloroquine reduces heart rate by modulating the hyperpolarization-activated current If: Novel electrophysiological insights and therapeutic potential. *Heart Rhythm* **12**, 2186-2194 (2015).

12. Huang BH, Wu CH, Hsia CP, Yin Chen C. Azithromycin-induced torsade de pointes. *Pacing Clin Electrophysiol* **30**, 1579-1582 (2007).

13. Ray WA, Murray KT, Hall K, Arbogast PG, Stein CM. Azithromycin and the Risk of Cardiovascular Death. *New England Journal of Medicine* **366**, 1881-1890 (2012).

14. Kezerashvili A, Khattak H, Barsky A, Nazari R, Fisher JD. Azithromycin as a cause of QT-interval prolongation and torsade de pointes in the absence of other known precipitating factors. *J Interv Card Electrophysiol* **18**, 243-246 (2007).

15. Rosenberg ES*, et al.* Association of Treatment With Hydroxychloroquine or Azithromycin With In-Hospital Mortality in Patients With COVID-19 in New York State. *JAMA* **323**, 2493-2502 (2020).

16. Wang G*, et al.* Mechanistic insights into ventricular arrhythmogenesis of hydroxychloroquine and azithromycin for the treatment of COVID-19. *bioRxiv*, 2020.2005.2021.108605 (2020).

17. Chorin E*, et al.* The QT interval in patients with COVID-19 treated with hydroxychloroquine and azithromycin. *Nat Med* **26**, 808-809 (2020).

18. Mercuro NJ*, et al.* Risk of QT Interval Prolongation Associated With Use of Hydroxychloroquine With or Without Concomitant Azithromycin Among Hospitalized Patients Testing Positive for Coronavirus Disease 2019 (COVID-19). *JAMA Cardiol* **5**, 1036-1041 (2020).

19. Saleh M*, et al.* Effect of Chloroquine, Hydroxychloroquine, and Azithromycin on the Corrected QT Interval in Patients With SARS-CoV-2 Infection. *Circ Arrhythm Electrophysiol* **13**, e008662 (2020).

20. Ramireddy A*, et al.* Experience With Hydroxychloroquine and Azithromycin in the Coronavirus Disease 2019 Pandemic: Implications for QT Interval Monitoring. *J Am Heart Assoc* **9**, e017144 (2020).

21. Karbassi E*, et al.* Cardiomyocyte maturation: advances in knowledge and implications for regenerative medicine. *Nat Rev Cardiol* **17**, 341-359 (2020).

22. Kolanowski TJ*, et al.* Enhanced structural maturation of human induced pluripotent stem cell-derived cardiomyocytes under a controlled microenvironment in a microfluidic system. *Acta Biomater* **102**, 273-286 (2020).

23. Huebsch N*, et al.* Automated Video-Based Analysis of Contractility and Calcium Flux in Human-Induced Pluripotent Stem Cell-Derived Cardiomyocytes Cultured over Different Spatial Scales. *Tissue Eng Part C Methods* **21**, 467-479 (2015).

24. King JH, Huang CL, Fraser JA. Determinants of myocardial conduction velocity: implications for arrhythmogenesis. *Front Physiol* **4**, 154 (2013).

25. Cavalcanti AB*, et al.* Hydroxychloroquine with or without Azithromycin in Mild-to-Moderate Covid-19. *N Engl J Med*, (2020).

26. Khuroo MS. Chloroquine and hydroxychloroquine in coronavirus disease 2019 (COVID-19). Facts, fiction and the hype: a critical appraisal. *Int J Antimicrob Agents* **56**, 106101 (2020).

27. Touret F*, et al.* In vitro screening of a FDA approved chemical library reveals potential inhibitors of

SARS-CoV-2 replication. *Sci Rep* **10**, 13093 (2020).

28. Durcan L, Clarke WA, Magder LS, Petri M. Hydroxychloroquine Blood Levels in Systemic Lupus Erythematosus: Clarifying Dosing Controversies and Improving Adherence. *J Rheumatol* **42**, 2092-2097 (2015).

29. Yao X*, et al.* In Vitro Antiviral Activity and Projection of Optimized Dosing Design of Hydroxychloroquine for the Treatment of Severe Acute Respiratory Syndrome Coronavirus 2 (SARS-CoV-2). *Clin Infect Dis* **71**, 732-739 (2020).

30. Jeong BH*, et al.* Peak Plasma Concentration of Azithromycin and Treatment Responses in Mycobacterium avium Complex Lung Disease. *Antimicrob Agents Chemother* **60**, 6076-6083 (2016).

31. Yang Z*, et al.* Azithromycin Causes a Novel Proarrhythmic Syndrome. *Circ Arrhythm Electrophysiol* **10**, (2017).

32. Zuckerman JM. The newer macrolides: azithromycin and clarithromycin. *Infect Dis Clin North Am* **14**, 449-462, x (2000).

33. Tett SE, Cutler DJ, Day RO, Brown KF. A dose-ranging study of the pharmacokinetics of hydroxy-chloroquine following intravenous administration to healthy volunteers. *Br J Clin Pharmacol* **26**, 303-313 (1988).

34. Zheng S, Matzneller P, Zeitlinger M, Schmidt S. Development of a population pharmacokinetic model characterizing the tissue distribution of azithromycin in healthy subjects. *Antimicrob Agents Chemother* **58**, 6675-6684 (2014).

35. Liu J*, et al.* Hydroxychloroquine, a less toxic derivative of chloroquine, is effective in inhibiting SARS-CoV-2 infection in vitro. *Cell Discov* **6**, 16 (2020).

36. Araujo FG, Shepard RM, Remington JS. In vivo activity of the macrolide antibiotics azithromycin, roxithromycin and spiramycin against Toxoplasma gondii. *Eur J Clin Microbiol Infect Dis* **10**, 519-524 (1991).

37. Kitani T*, et al.* Human-Induced Pluripotent Stem Cell Model of Trastuzumab-Induced Cardiac Dysfunction in Patients With Breast Cancer. *Circulation* **139**, 2451-2465 (2019).

38. Takeda A*, et al.* Macrolide antibiotics enhance the antitumor effect of lansoprazole resulting in lysosomal membrane permeabilizationassociated cell death. *Int J Oncol* **57**, 1280-1292 (2020).

39. Mukai S*, et al.* Macrolides sensitize EGFR-TKI-induced non-apoptotic cell death via blocking autophagy flux in pancreatic cancer cell lines. *Int J Oncol* **48**, 45-54 (2016).

40. Lindner D*, et al.* Association of Cardiac Infection With SARS-CoV-2 in Confirmed COVID-19 Autopsy Cases. *JAMA Cardiol* **5**, 1281-1285 (2020).

41. Bailey AL*, et al.* SARS-CoV-2 Infects Human Engineered Heart Tissues and Models COVID-19 Myocarditis. *JACC Basic Transl Sci* **6**, 331-345 (2021).

42. Perez-Bermejo JA*, et al.* SARS-CoV-2 infection of human iPSC-derived cardiac cells reflects cytopathic features in hearts of patients with COVID-19. *Sci Transl Med* **13**, (2021).

43. Mills RJ*, et al.* BET inhibition blocks inflammation-induced cardiac dysfunction and SARS-CoV-2 infection. *Cell* **184**, 2167-2182 e2122 (2021).

44. Norinder U, Tuck A, Norgren K, Munic Kos V. Existing highly accumulating lysosomotropic drugs with potential for repurposing to target COVID-19. *Biomed Pharmacother* **130**, 110582 (2020).

45. Scherrmann JM. Intracellular ABCB1 as a Possible Mechanism to Explain the Synergistic Effect of Hydroxychloroquine-Azithromycin Combination in COVID-19 Therapy. *AAPS J* **22**, 86 (2020).

46. Cyganek L*, et al.* Deep phenotyping of human induced pluripotent stem cell-derived atrial and ventricular cardiomyocytes. *JCI Insight* **3**, (2018).

47. Feyen DAM*, et al.* Metabolic Maturation Media Improve Physiological Function of Human iPSC-Derived Cardiomyocytes. *Cell Rep* **32**, 107925 (2020).

48. Laing JG, Tadros PN, Green K, Saffitz JE, Beyer EC. Proteolysis of connexin43-containing gap junctions in normal and heat-stressed cardiac myocytes. *Cardiovasc Res* **38**, 711-718 (1998).

49. Mauthe M*, et al.* Chloroquine inhibits autophagic flux by decreasing autophagosome-lysosome fusion. *Autophagy* **14**, 1435-1455 (2018).

50. Streckfuss-Bomeke K*, et al.* Comparative study of human-induced pluripotent stem cells derived from bone marrow cells, hair keratinocytes, and skin fibroblasts. *European heart journal* **34**, 2618-2629 (2013).

51. Rossler U*, et al.* Efficient generation of osteoclasts from human induced pluripotent stem cells and functional investigations of lethal CLCN7-related osteopetrosis. *J Bone Miner Res* **36**, 1621-1635 (2021).

52. Li W*, et al.* Establishment of an automated patch-clamp platform for electrophysiological and pharmacological evaluation of hiPSC-CMs. *Stem Cell Res* **41**, 101662 (2019).

53. Luo X*, et al.* IP3R-Mediated Compensatory Mechanism for Calcium Handling in Human Induced Pluripotent Stem Cell-Derived Cardiomyocytes With Cardiac Ryanodine Receptor Deficiency. *Front Cell Dev Biol* **8**, 772 (2020).

54. QuoData. Quality & Statistics GmbH, https://quodata.de/, accessed 08/19/2021.

907 55. McQuin C*, et al.* CellProfiler 3.0: Next-generation image processing for biology. *PLoS Biol* **16**,
908 e2005970 (2018).

909

910 56. Schindelin J*, et al.* Fiji: an open-source platform for biological-image analysis. *Nat Methods* **9**, 676-
911 682 (2012).

912

913 57. Li W*, et al.* Disease Phenotypes and Mechanisms of iPSC-Derived Cardiomyocytes From Brugada
914 Syndrome Patients With a Loss-of-Function SCN5A Mutation. *Front Cell Dev Biol* **8**, 592893 (2020).

915

916

Supplementary information

Figure S1

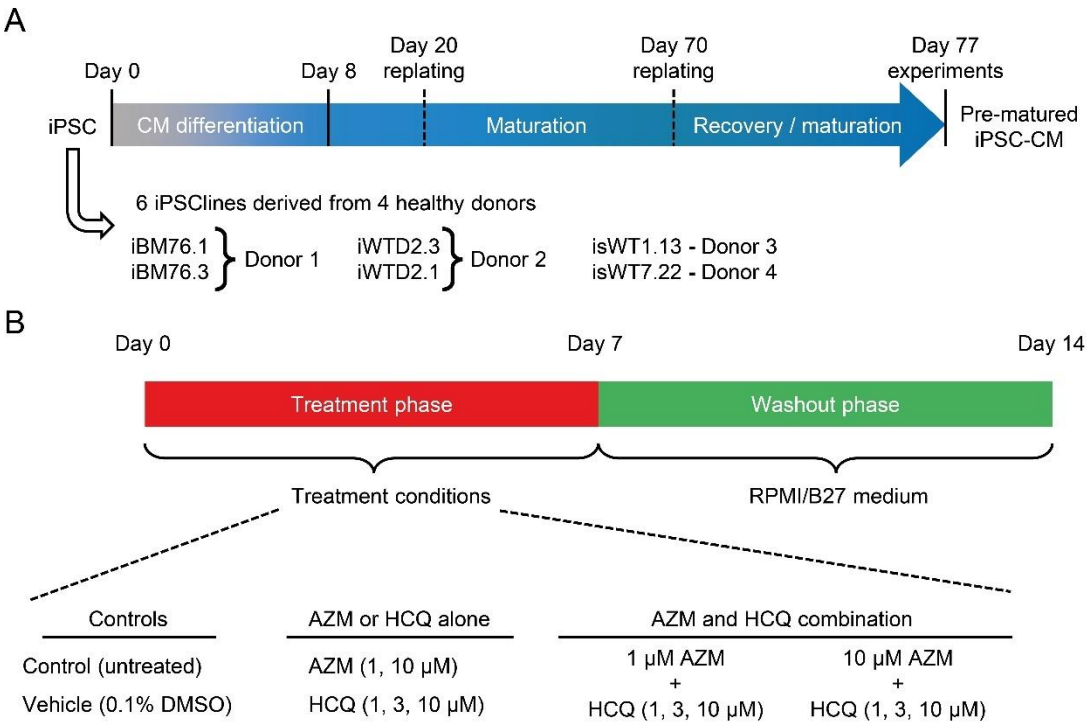

Supplementary Figure 1: Experimental scheme. A, Timeline of iPSC-CM differentiation and maturation under long-term cultivation for 77 days before the drug treatment and functional analysis. iPSC lines derived from 4 healthy donors were used in the experiments to consider different genetic background. B, Scheme of all conditions used in the study with drug treatment and washout phases.

Figure S2

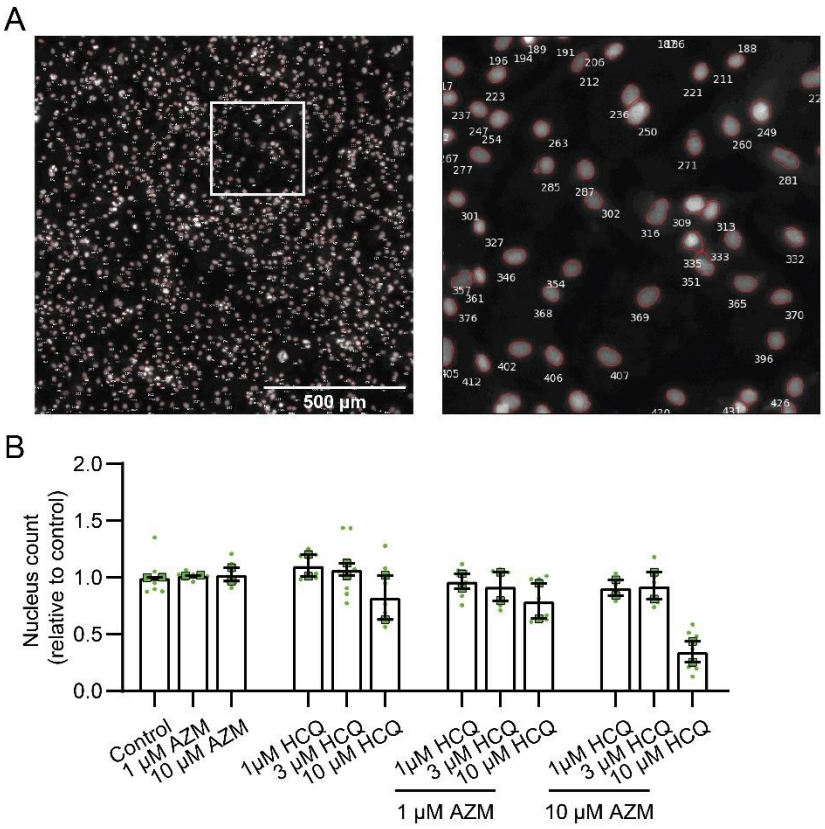

Supplementary Figure 2: Quantification of nucleus number after 7-day treatment with the drugs. A, Representative images of iPSC-CMs stained with Hoechst33342 and nucleus count using CellProfiler software. B, Nucleus counts after the 7-day drug treatment relative to the control group (n = 7-8 images from 2 independent experiments). Data represent mean and SEM of n = 2 different iPSC-CM differentiations from healthy donor iBM76.

Figure S3

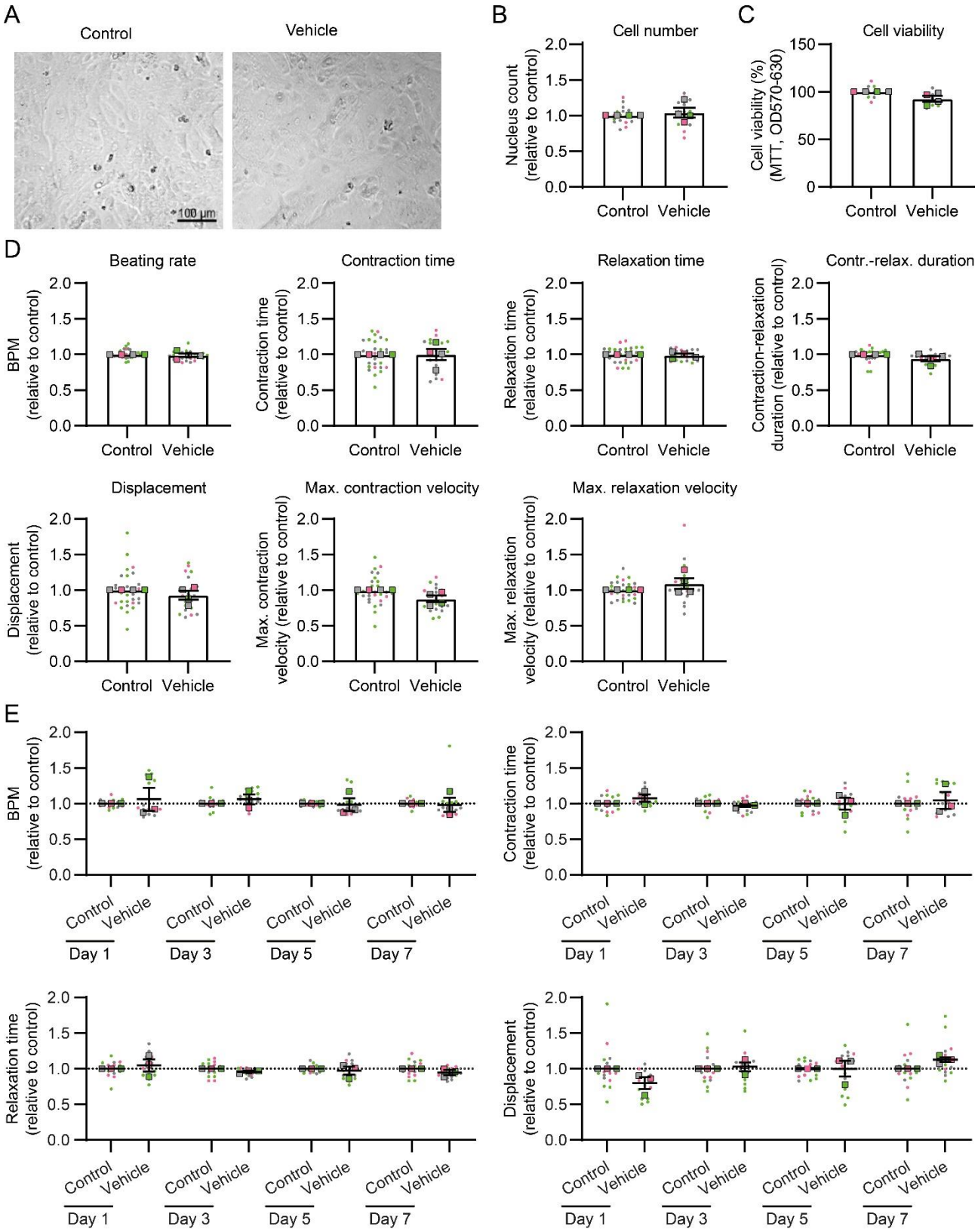

Supplementary Figure 3: Cell viability and contractility in vehicle (0.1% DMSO) treated iPSC-CMs. A, Brightfield images of iPSC-CMs after 7-day culture with RPMI/B27 medium (control) or in the presence of 0.1% DMSO vehicle showing that vehicle treatment did not affect CM morphology.

B, Cell density was investigated based on the quantification of cell nucleus counts using Hoechst33342 staining and fluorescence imaging. C, Cell viability examined by MTT assay. D, Quantification of contractile function using video-based motion vector analysis. Data represent mean and SEM of n = 4 different iPSC-CM differentiations from 3 healthy donors indicated by different colours (iBM76.3 in green, iWTD2.1 in grey, isWT7.22 in pink). Points show technical replicates and squares represent mean values. E, Changes in beating parameters over time. Pooled individual replicates from n = 3 different iPSC-CM differentiations (iBM76.3 in green, iWTD2.1 in grey, isWT7.22 in pink).

Figure S4

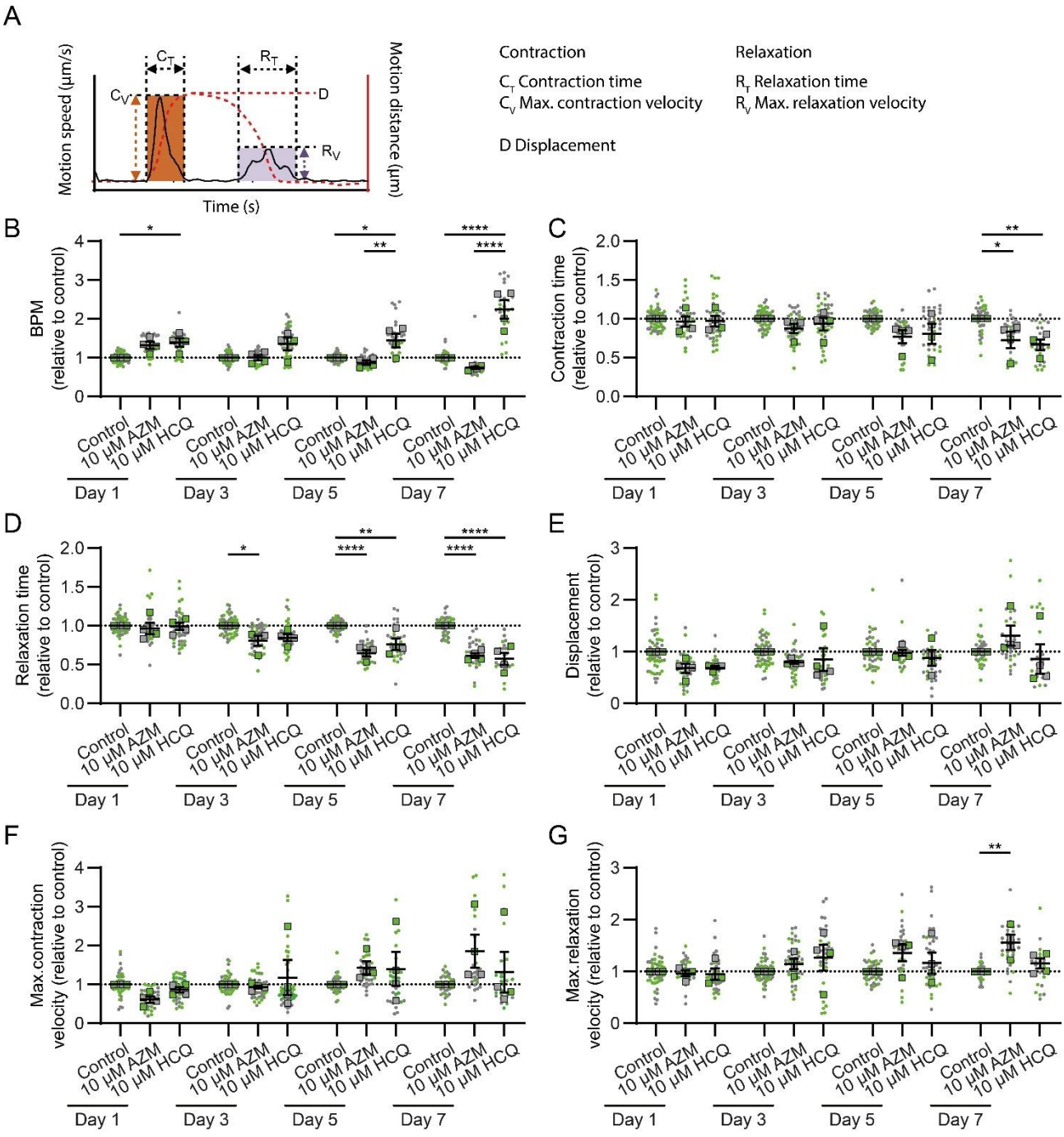

Supplementary Figure 4: Effects of AZM and HCQ treatments on contraction parameters. A, Scheme of beating trace and calculated parameters using Maia motion analysis software. B-G, Effects of 10 µM AZM and 10 µM HCQ during the treatment period of 7 days. Shown are data of the beating rate (B), contraction time (C), relaxation time (D), displacement (E), max. contraction velocity (F) and max. relaxation velocity (G) which were normalized to the control. Points represent technical replicates and squares depict the means of individual experiments using iPSC-CM from 3 healthy donors indicated by different colors (iBM76.3 in green, iWTD2.1 in grey, isWT7.22 in pink). Lines indicate overall mean. n = 26-54 videos from 4-5 experiments were analyzed per group.

Statistical analysis was performed based on the mean values of the individual experiments using two-way ANOVA and Tukey's multiple comparison test. * $p < 0.05$, ** $p < 0.01$, *** $p < 0.001$, **** $p < 0.0001$.

Figure S5

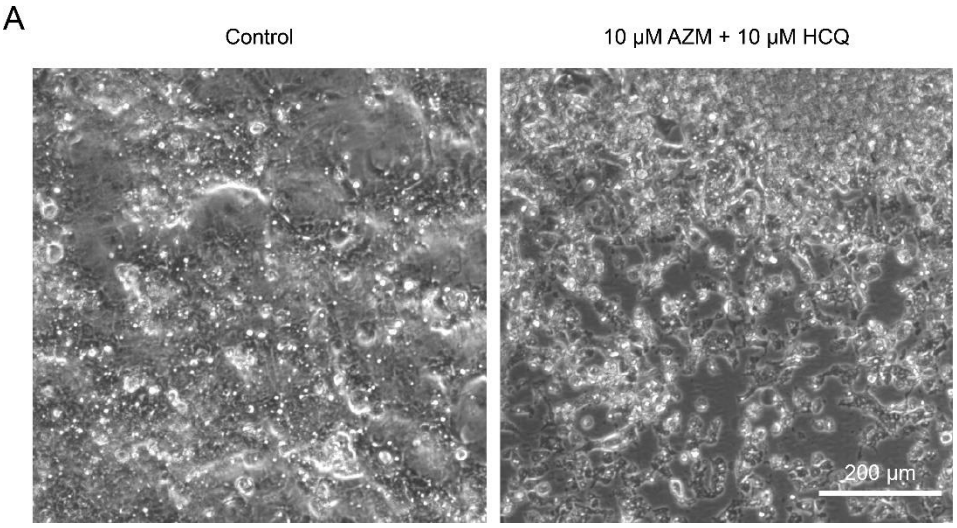

Supplementary Figure 5: Representative images of iPSC-CMs on MEA plate. A, B, Morphology of iPSC-CMs in the vehicle treated (A) and 10 µM AZM and 10 µM HCQ treated (B) groups at day 8. Combination treatment with 10 µM AZM and 10 µM HCQ increased the number of dead cells.

Figure S6

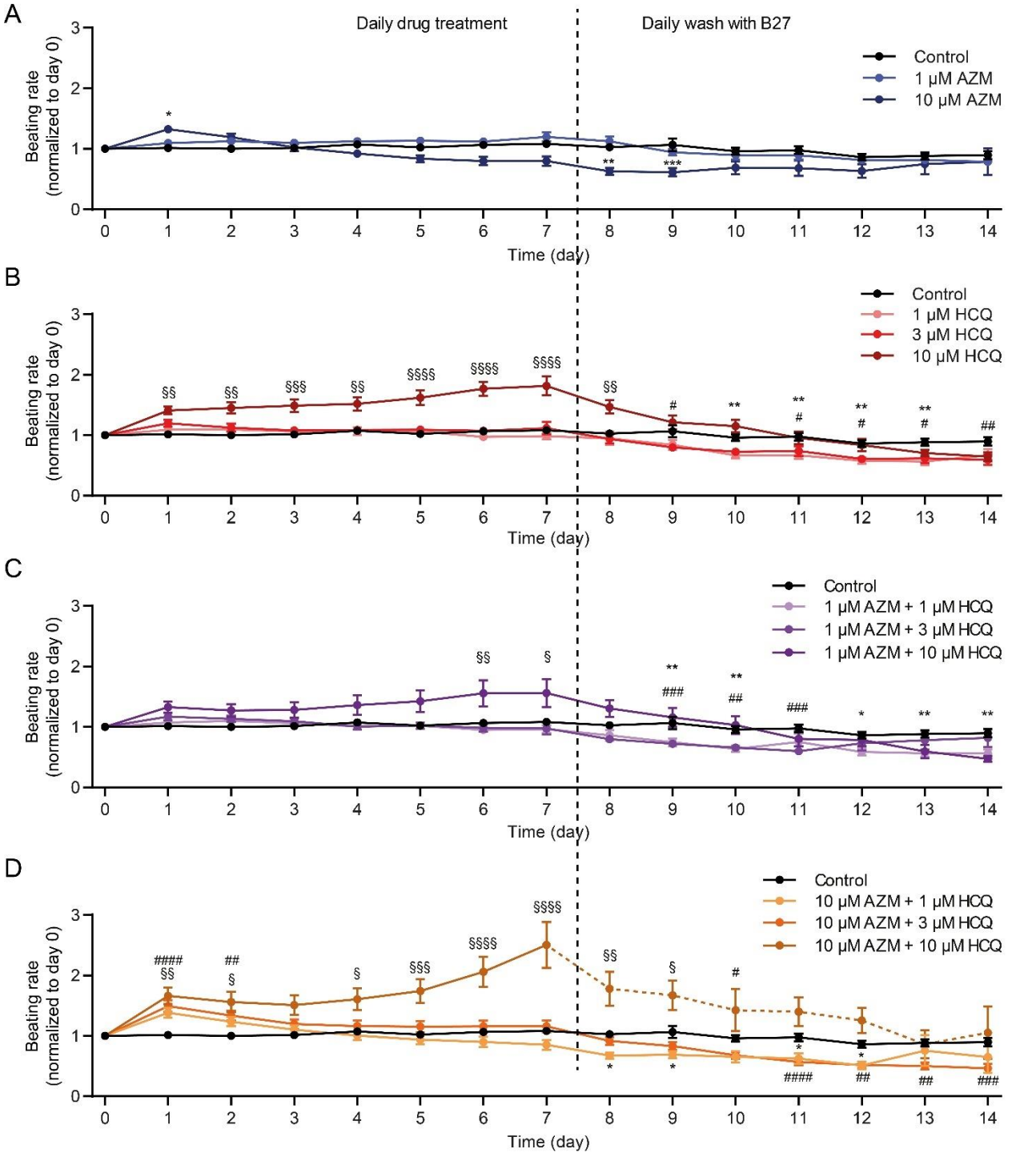

Supplementary Figure 6: Effects of HCQ and AZM treatments on the beating rates of iPSC-CMs. A, Effect of AZM treatment (1 and 10 μM) on spontaneously beating rates (normalized to day 0) during 7-day drug treatment (left) and following 7-day washout (right). B, Effect of HCQ treatment (1, 3 and 10 μM) on spontaneously beating rates during 7-day drug treatment (left) and following 7-day washout (right). C, Effect of HCQ (1, 3, and 10 μM) combined with 1 μM AZM on spontaneous beating rates during 7-day drug treatment (left) and following 7-day washout (right). D, Effect of HCQ (1, 3, and 10 μM) combined with 10 μM AZM on spontaneously beating rates

969 during 7-day drug treatment (left) and following 7-day washout (right). iPSC-CMs derived from four
970 donors were used for MEA recording. For the initial recording (day 0), $10 \leq n \leq 13$ for all conditions.
971 Numbers of beating iPSC-CM cultures used for the analysis are listed in Supplementary Table 1.
972 Two-way ANOVA with Bonferroni post-hoc test (* $p < 0.05$, ** $p < 0.01$, *** $p < 0.001$, and **** $p <$
973 0.0001).
974
975
976

Figure S7

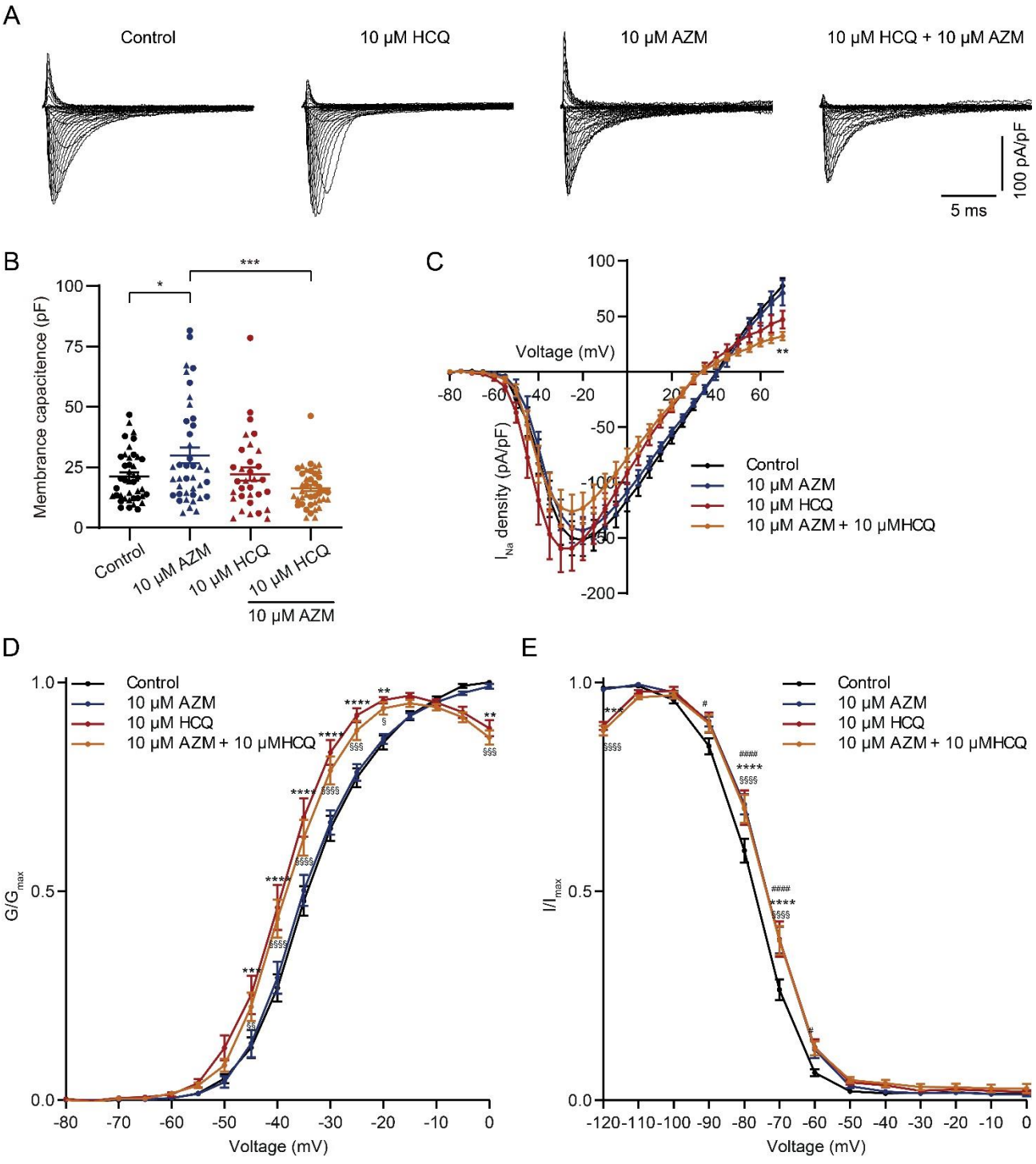

Supplementary Figure 7: Effects of HCQ and AZM on the sodium channel. A, Representative I_{Na} traces of iPSC-CMs in the control and drug-treated groups (10 μM AZM, 10 μM HCQ, and their combination). B, Statistical analysis of membrane capacitance of iPSC-CMs in the control and drug-treated groups. Different shapes of symbols indicate different differentiations. C, Statistical analysis of I_{Na} in control and 7-day drug-treated groups. D, E Steady-state activation (D) and inactivation (E) in control and 7-day drug treated groups. I_{Na} steady-state kinetics are altered by AZM and HCQ. n=41, 40, 30, and 41 cells for the control, 10 μM AZM-treated, 10 μM HCQ-treated,

and AZM and HCQ combination groups, respectively, were analyzed; shown are mean and SEM from 6 independent differentiations (B-E). One-way ANOVA with Tukey's multiple comparison test (B) and two-way ANOVA with Bonferroni post-hoc test (C-E) were used for statistical analysis (* $p < 0.05$, ** $p < 0.01$, *** $p < 0.001$, and **** $p < 0.001$).

Supplementary Table 1: Spontaneously beating status of iPSC-CM culture during 15 days of the recording

Number of beating culture	Day 0	Day 1	Day 2	Day 3	Day 4	Day 5	Day 6	Day 7	Day 8	Day 9	Day 10	Day 11	Day 12	Day 13	Day 14
Basal	13	13	13	13	13	13	13	13	13	13	13	13	13	13	13
1 µM AZM	10	10	10	10	10	10	10	10	10	10	10	10	10	10	10
10 µM AZM	11	11	11	11	11	11	11	11	11	11	9	9	9	9	9
1 µM HCQ	10	10	10	10	10	10	10	10	10	10	9	8	8	8	8
3 µM HCQ	10	10	10	10	10	10	10	10	10	10	10	10	9	9	8
10 µM HCQ	12	12	12	12	12	12	12	12	12	12	11	11	10	8	6
1 µM AZM & 1 µM HCQ	10	10	10	10	10	10	10	10	10	10	10	10	9	9	9
1 µM AZM & 3 µM HCQ	11	11	11	11	11	11	11	11	11	11	10	9	8	8	8
1 µM AZM & 10 µM HCQ	11	11	11	11	11	11	11	11	11	11	11	10	8	6	6
10 µM AZM & 1 µM HCQ	11	11	11	11	11	11	11	11	11	11	10	9	9	9	9
10 µM AZM & 3 µM HCQ	11	11	11	11	11	11	11	11	11	11	11	11	8	8	6
10 µM AZM & 10 µM HCQ	11	11	11	11	11	11	11	8	5	4	4	3	2	2	2

Supplementary Video

Supplementary Video 1

https://cloudstore.zih.tu-dresden.de/index.php/s/aTgmHiBpzbSLAHf

Supplementary Video 2

https://cloudstore.zih.tu-dresden.de/index.php/s/CN55aXTJPQL6f5H